Inhibition of mitochondrial translation overcomes venetoclax resistance in AML through activation of the integrated stress response

David Sharon[1], Severine Cathelin[1], Sara Mirali[1], Justin M. Di Trani[2], David J. Yanofsky[2,3], Kristine A. Keon[2,3], John L. Rubinstein[2,3], Aaron D. Schimmer[1,3], Troy Ketela[1], Steven M. Chan[1,3]*

Venetoclax is a specific B cell lymphoma 2 (BCL-2) inhibitor with promising activity against acute myeloid leukemia (AML), but its clinical efficacy as a single agent or in combination with hypomethylating agents (HMAs), such as azacitidine, is hampered by intrinsic and acquired resistance. Here, we performed a genome-wide CRISPR knockout screen and found that inactivation of genes involved in mitochondrial translation restored sensitivity to venetoclax in resistant AML cells. Pharmacologic inhibition of mitochondrial protein synthesis with antibiotics that target the ribosome, including tedizolid and doxycycline, effectively overcame venetoclax resistance. Mechanistic studies showed that both tedizolid and venetoclax suppressed mitochondrial respiration, with the latter demonstrating inhibitory activity against complex I [nicotinamide adenine dinucleotide plus hydrogen (NADH) dehydrogenase] of the electron transport chain (ETC). The drugs cooperated to activate a heightened integrated stress response (ISR), which, in turn, suppressed glycolytic capacity, resulting in adenosine triphosphate (ATP) depletion and subsequent cell death. Combination treatment with tedizolid and venetoclax was superior to either agent alone in reducing leukemic burden in mice engrafted with treatment-resistant human AML. The addition of tedizolid to azacitidine and venetoclax further enhanced the killing of resistant AML cells in vitro and in vivo. Our findings demonstrate that inhibition of mitochondrial translation is an effective approach to overcoming venetoclax resistance and provide a rationale for combining tedizolid, azacitidine, and venetoclax as a triplet therapy for AML.

INTRODUCTION

Acute myeloid leukemia (AML) is an aggressive hematologic malignancy characterized by the accumulation of immature myeloid cells defective in their maturation and function. Standard-of-care treatment for most patients involves intensive induction chemotherapy followed by additional courses of chemotherapy for patients with lower-risk disease or an allogeneic bone marrow (BM) transplant for higher-risk patients (1). Even with these aggressive treatments, 5-year overall survival is between 30 and 40% and much lower for those over age 65 (2). Moreover, patients with advanced age and/or multiple medical comorbidities often do not tolerate these high-intensity treatments, highlighting the need for more effective and less toxic AML therapies.

Antiapoptotic proteins in the B cell lymphoma 2 (BCL-2) family, most notably BCL-2 and myeloid cell leukemia 1 (MCL-1), promote the survival of AML cells by counteracting the proapoptotic activity of proteins such as BCL-2–like protein 11 (BCL2L11, also known as BIM) (3, 4). Venetoclax is a small-molecule BCL-2 homology domain-3 (BH3) mimetic that specifically disrupts the binding between the BH3 domain of proapoptotic proteins, such as BIM, and the hydrophobic cleft of BCL-2 (5). This disruption unleashes the activation of multi-domain proapoptotic proteins, including BCL2-associated X protein (BAX) and BCL2 antagonist/killer 1 (BAK), which, in turn, triggers the intrinsic apoptotic pathway through mitochondrial outer membrane permeabilization (6).

Venetoclax has demonstrated activity against a range of solid and hematologic malignancies. In preclinical studies, venetoclax induced apoptosis in a variety of AML cell lines and primary cells including leukemic stem cells (LSCs) in vitro and in mouse xenografts (7–9). These findings prompted a phase 2 clinical trial of venetoclax monotherapy in patients with relapsed/refractory AML. The overall response rate was only 19% (6 of 32 patients) with a median time to progression of 2.5 months (10). These findings underscore the importance of understanding the mechanisms of resistance and developing combination therapies to circumvent them.

The best-described mechanism of venetoclax resistance is through increased expression of functionally redundant antiapoptotic proteins in the BCL-2 family, with MCL-1 being the most commonly implicated protein. Pharmacologic and genetic approaches that either directly or indirectly suppress MCL-1 function can overcome resistance to BCL-2 inhibition (11–15). However, a variety of normal tissues also express high amounts of MCL-1 and are dependent on its activity for survival. For instance, MCL-1 has an obligate role in maintaining the survival and self-renewal function of hematopoietic stem cells (16, 17). MCL-1 also promotes the viability of cardiomyocytes and hepatocytes in conditional knockout mouse models (18, 19). Therefore, suppression of MCL-1 carries the risk of profound toxicity to normal tissues, which would be further exacerbated by concurrent BCL-2 inhibition, translating to a potentially narrow or absent therapeutic window in patients.

Alternative strategies involving the combination of venetoclax with hypomethylating agents (HMAs) or low-dose cytarabine (LDAC) have demonstrated promising activity in early phase clinical trials. In an early phase study of venetoclax in combination with HMAs (decitabine or azacitidine) in elderly patients with previously untreated AML, 67% of patients achieved a complete remission (CR)

[1]Princess Margaret Cancer Centre, Toronto, Ontario M5G 1L7, Canada. [2]Molecular Medicine Program, The Hospital for Sick Children, Toronto, Ontario M5G 0A4, Canada. [3]Department of Medical Biophysics, University of Toronto, Toronto, Ontario M5G 1L7, Canada.
*Corresponding author. Email: steven.chan@uhnresearch.ca

Sharon et al., Sci. Transl. Med. 11, eaax2863 (2019)   30 October 2019

1 of 15

or CR with incomplete hematologic recovery (CRi), with a median duration of response of 11.3 months (20). Treatment with venetoclax in combination with LDAC resulted in a CR/CRi rate of 54% and a median duration of response of 8.1 months (21). These results led to the U.S. Food and Drug Administration (FDA) approval of venetoclax in combination with HMAs or LDAC for the treatment of newly diagnosed elderly patients with AML who are not eligible for intensive induction chemotherapy. However, intrinsic and acquired resistance was still a common feature that limited the clinical benefit of these combinations. Furthermore, in a retrospective analysis of patients with relapsed and refractory AML treated with venetoclax in combination with HMAs or LDAC, the objective response rate was only 21% (9 of 43 patients) (22). Thus, there is an unmet need to improve the clinical efficacy of venetoclax combinations in the treatment of AML.

To address the above issues, we sought to identify an alternative approach to overcoming venetoclax resistance. We performed an unbiased genome-wide CRISPR knockout screen to find genes that, upon inactivation, restored sensitivity to venetoclax in an AML cell line with acquired resistance. This screen identified multiple genes encoding components of the mitochondrial translation machinery and led us to investigate whether pharmacologic inhibition of mitochondrial translation can circumvent venetoclax resistance. Here, we determined the efficacy of this approach using AML cell line models, as well as primary patient samples, and investigated the mechanisms that mediate this effect.

RESULTS

Mitochondrial translation is a target for overcoming venetoclax resistance

We first generated a panel of highly resistant AML clones by culturing MOLM13 and MV4-11 AML cells that are intrinsically sensitive to venetoclax [half maximal inhibitory concentration (IC_{50}) < 50 nM] in slowly escalating concentrations of the drug (up to 2000 nM) over a period of 2 months. We transduced the resistant cells with a lentiviral construct expressing a codon-optimized version of the *Streptococcus pyogenes* CRISPR-associated protein 9 (Cas9) endonuclease and a green fluorescent protein (GFP) marker. We generated clones by expanding individual fluorescence-activated cell sorting (FACS)–sorted GFP+ cells (Fig. 1A). The resulting clones were highly resistant to venetoclax (IC_{50} > 1000 nM) (fig. S1A). The resistant MOLM13 and MV4-11 clones expressed higher amounts of MCL-1 and BCL-2–like protein 1 (BCL2L1, also known as BCL-X_L), respectively, compared with their sensitive parental cells (fig. S1B). We did not identify a glycine-to-valine mutation at amino acid position 101 ($Gly^{101}Val$) in the *BCL-2* gene of resistant AML clones (fig. S1C). This mutation has previously been shown to confer resistance to venetoclax in chronic lymphocytic leukemia (23).

Next, we transduced one of the expanded clones (MOLM13-R1) with a pooled lentiviral single-guide RNA (sgRNA) library (Toronto KnockOut CRISPR Library—version 1—90k library) that targeted 17,661 protein-coding genes with 91,320 unique sgRNA sequences (~6 sgRNAs per gene) (24). Transduced cells were selected in puromycin and subsequently divided into two populations on day 0. One population was treated with venetoclax at 400 nM, a concentration that would trigger massive apoptosis in sensitive MOLM13 cells (fig. S1A). The other population was treated with dimethyl sulfoxide (DMSO) as control (Fig. 1A). The transduced cells were cultured for 29 days to negatively select sgRNAs that resensitized resistant

cells to venetoclax. Cell samples were collected on days 0, 8, 16, 22, and 29 and subjected to next-generation sequencing of the sgRNA target region to quantify the abundance of each construct.

We applied the Model-based Analysis of Genome-wide CRISPR-Cas9 Knockout (MAGeCK) algorithm to identify sgRNAs that were negatively and positively selected in the presence of venetoclax (25). Four of the top 10 ranked negatively selected genes [death-associated protein 3 (*DAP3*) (26), mitochondrial ribosomal protein L54 (*MRPL54*) (27), mitochondrial ribosomal protein L17 (*MRPL17*) (27), and ribosome binding factor A (*RBFA*) (28)] on day 8 encoded components of the mitochondrial translation machinery (Fig. 1B, left). The top-ranked positively selected gene was *BAX*, which encodes a key downstream mediator of apoptosis (29), indicating that even in the setting of high baseline resistance, its silencing could confer additional survival advantage (Fig. 1B, right). We next performed gene ontology enrichment analysis on the ranked list of negatively selected genes and found that process terms related to mitochondrial translation and component terms related to mitochondrial ribosomes were highly enriched (Fig. 1C). Furthermore, we observed a progressive decline in the abundance of each sgRNA over time in the presence of venetoclax (Fig. 1D). To confirm these findings, we transduced MOLM13-R1 cells with lentiviral vectors encoding two short hairpin RNAs (shRNAs) against *DAP3*, which encodes a protein in the small 28*S* mitoribosome subunit (26) and observed an increase in venetoclax sensitivity in the transduced population (Fig. 1E and fig. S1D). These findings suggest that inhibition of mitochondrial translation is a potential strategy for overcoming venetoclax resistance.

Protein synthesis inhibitor antibiotics overcome venetoclax resistance

To determine whether pharmacologic inhibition of mitochondrial translation could reproduce the above findings, we took advantage of a well-described off-target effect of antibiotics that block bacterial protein synthesis. Because of the evolutionarily conserved similarities between bacterial and mitochondrial ribosomes, this class of antibiotics has the potential to interfere with mitochondrial translation (30, 31). We determined the effects of five different FDA-approved antibiotics in this class on venetoclax sensitivity in MOLM13-R1 cells. We tested the antibiotics at their corresponding IC_{10} to maximize the suppressive effect on mitochondrial translation without causing excessive single-agent toxicity that would otherwise obscure the resensitization effect. Treatment with this class of antibiotics, with the exception of chloramphenicol, decreased the IC_{50} of venetoclax to ~30 nM, a value comparable to that of sensitive parental cells (Fig. 2A and fig. S1A). To confirm that the antibiotics blocked mitochondrial protein synthesis, we treated MOLM13-R1 cells with each antibiotic for 2 days followed by intracellular staining for subunit 1 of cytochrome C oxidase (MT-CO1), which is mitochondrially encoded, and subunit A of succinate dehydrogenase (SDHA), which is nuclear encoded (32, 33); a reduction in the ratio of MT-CO1 to SDHA staining correlates with mitochondrial translation inhibition. Tedizolid, an oxazolidinone-class antibiotic, and doxycycline, a tetracycline analog, were the two most effective antibiotics in suppressing mitochondrial protein synthesis (Fig. 2B). In addition to MT-CO1, tedizolid treatment reduced the expression of subunit 2 of cytochrome C oxidase (MT-CO2), another mitochondrially encoded protein, but not cytochrome C oxidase subunit IV (COX IV) or subunit B of succinate dehydrogenase, which are nuclear encoded (fig. S2A). Chloramphenicol at the concentration tested had no apparent impact on mitochondrial protein synthesis within the time frame
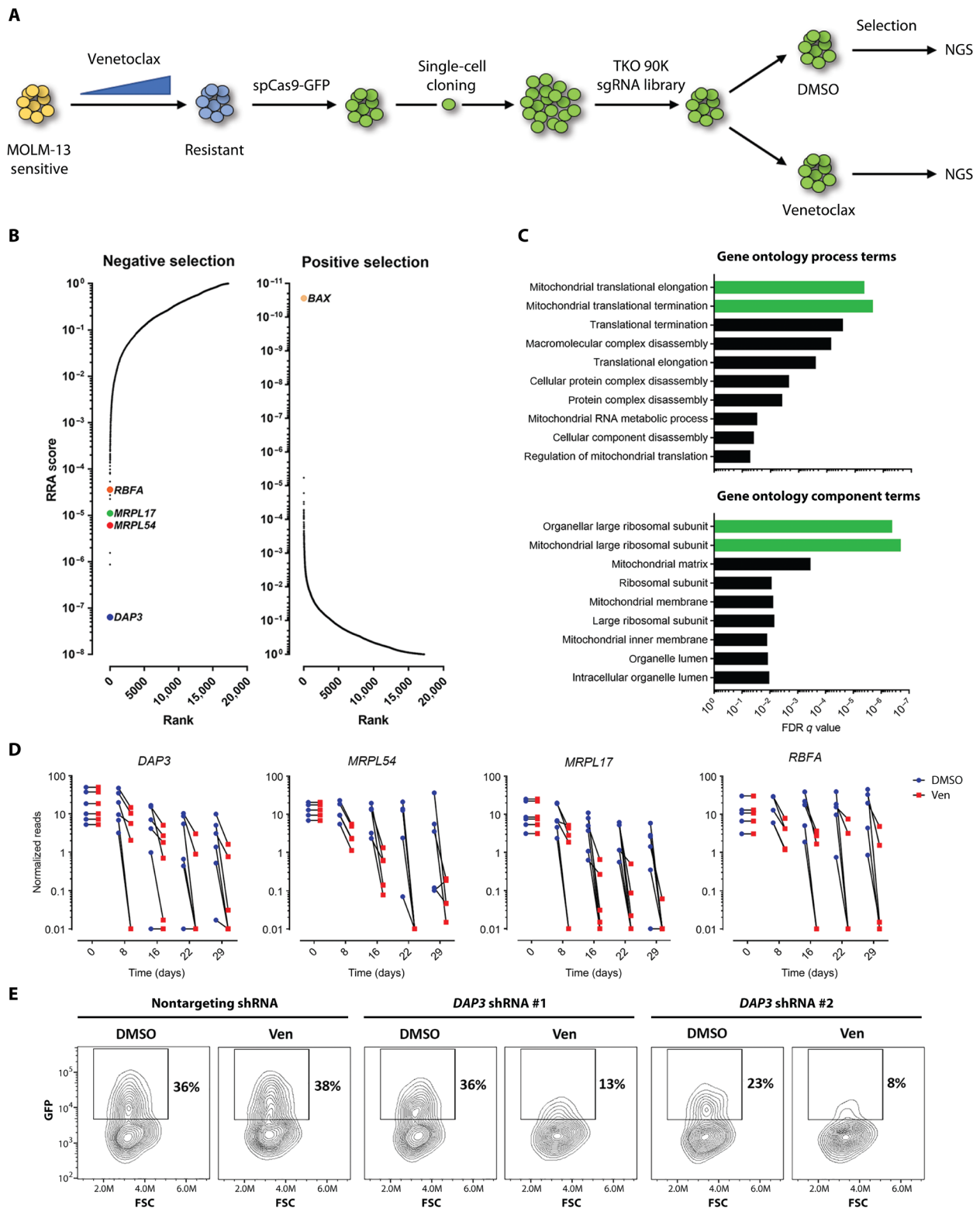
Fig. 1. CRISPR screen identifies mitochondrial translation as a target for overcoming venetoclax resistance in AML. (**A**) Schematic diagram depicting the experimental design of the genome-wide CRISPR knockout screen to identify genes that, upon inactivation, restore sensitivity to venetoclax. (**B**) Negatively and positively selected genes identified by the CRISPR knockout screen. Genes are ranked on the basis of the robust rank aggregation (RRA) score as calculated by the MAGeCK algorithm. (**C**) Gene ontology enrichment analysis of the top-ranked negatively selected genes. (**D**) Normalized number of sequencing reads of each gRNA construct targeting the indicated gene at different time points in cells cultured in DMSO (vehicle) or venetoclax (400 nM). (**E**) Percentage of transduced MOLM13-R1 cells (GFP⁺) expressing the indicated shRNAs after treatment with DMSO (vehicle) or venetoclax (400 nM) for 5 days. Representative data of three technical replicates. FSC, forward scatter.

Fig. 2. Pharmacological inhibition of mitochondrial translation overcomes resistance to venetoclax in AML. (**A**) Viability of MOLM13-R1 cells treated with serial dilutions of venetoclax for 5 days in the absence or presence of one of the indicated antibiotics. $n = 3$ technical replicates. (**B**) Normalized ratio of MT-COI to SDHA expression in MOLM13-R1 cells after treatment with the indicated antibiotic for 2 days. $n = 3$ technical replicates. (**C**) Viability of venetoclax-resistant MOLM13 and MV4-11 cells after treatment with DMSO (vehicle), venetoclax alone (500 nM), tedizolid alone (5 μM), or a combination of the two drugs over the course of 6 days. $n = 3$ technical replicates. (**D**) Viability of resistant OCI-AML2 and OCI-AML3 cells after treatment with DMSO (vehicle), venetoclax alone (500 nM), doxycycline alone (2.5 μg/ml), tedizolid alone (5 μM), or combination of venetoclax with tedizolid or doxycycline for 3 days. $n = 3$ technical replicates. (**E**) Percentage of CD34+ cells in two primary AML samples (8227 and 130578) and cord blood HSPCs after treatment with vehicle, doxycycline alone (7.5 μg/ml), venetoclax alone (1 μM), or a combination of the two drugs for 24 hours. Representative data of $n = 3$ biological replicates. Data shown are means ± SEM. Statistical significance was determined by ANOVA. *$P \le 0.05$.
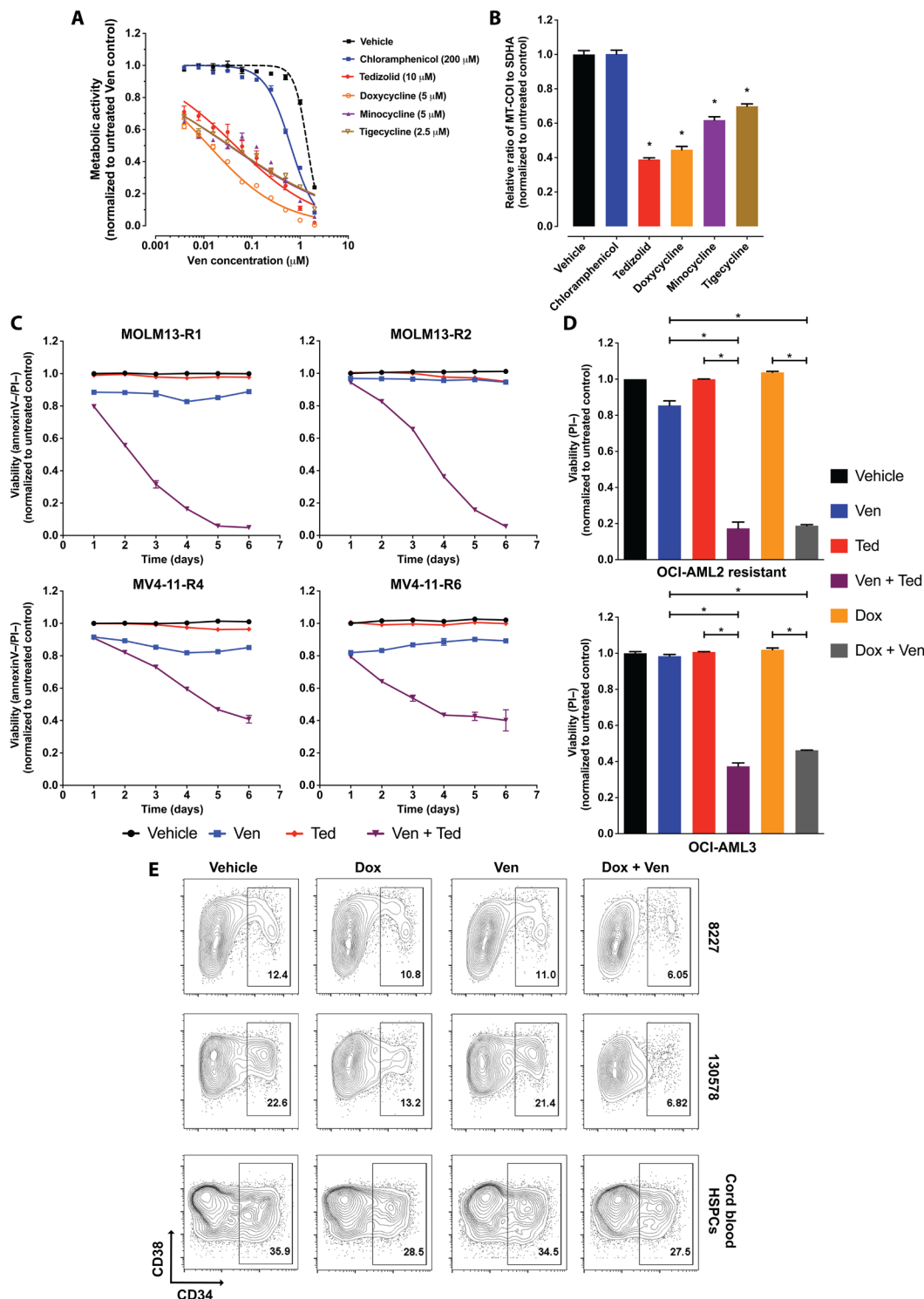
of the experiment (Fig. 2B); this correlated with only a modest increase in venetoclax sensitivity (Fig. 2A). We focused our subsequent studies on tedizolid and doxycycline because of their superior efficacy in suppressing mitochondrial translation compared with the other antibiotics.

To confirm that this effect was not restricted to MOLM13-R1, we tested the impact of tedizolid on venetoclax sensitivity in other resistant cell line models derived from MOLM13 (clone MOLM13-R2) and MV4-11 (clones MV4-11-R4 and R6). The cells were treated with venetoclax alone, tedizolid alone, or both drugs, and their viability was monitored daily by annexin V and propidium iodide (PI) staining over a period of 6 days. We observed a progressive decline in cell viability only with combination treatment but not with each drug alone (Fig. 2C). Note that the MOLM13-resistant clones overexpressed MCL-1, whereas the MV4-11 clones overexpressed BCL-X$_L$ (fig. S1B), suggesting that combination treatment is effective regardless of which antiapoptotic protein is overexpressed. We observed a similar response to tedizolid or doxycycline in combination with venetoclax in OCI-AML-2 cells with acquired resistance and OCI-AML-3 cells, which are intrinsically resistant to venetoclax (Fig. 2D). Tedizolid treatment also sensitized parental and resistant MOLM13 cells to another BCL-2 inhibitor,

S55746, which is structurally distinct from venetoclax (fig. S2B) (*34*). Tedizolid had minimal impact on sensitivity to pharmacologic MCL-1 and BCL-X$_L$ inhibition in venetoclax-resistant cells, indicating that its effect was specific for BCL-2 inhibition (fig. S2, C and D). Our results demonstrate that pharmacologic inhibition of mitochondrial translation effectively overcomes intrinsic and acquired resistance to venetoclax in AML cell lines.

Although conventional therapies are often effective in eliminating the leukemic bulk, a small population of LSCs frequently persists and contributes to disease relapse (*35*). Therapies that target LSCs may reduce the risk of relapse. To determine whether the effects of antibiotics on venetoclax sensitivity extended to LSCs, we took advantage of two primary human AML samples (8227 and 130578) that can be maintained and expanded in serum-free medium supplemented with cytokines for prolonged periods. Each sample was characterized by four distinct subpopulations defined by CD34 and CD38 expression, and LSC activity as assayed by xenotransplantation was restricted to the CD34$^+$ fractions (table S1) (*36*). The CD34/CD38 profile and hierarchical organization were maintained during long-term ex vivo culture, thus enabling the analysis of differences in drug sensitivities between LSC-enriched and non-LSC populations (fig. S3A) (*36*). We treated the AML samples with venetoclax alone, doxycycline alone, or a combination of the two drugs for 24 hours and analyzed the size of the CD34$^+$ fraction after treatment. Doxycycline was used instead of tedizolid for experiments involving primary samples because the cells were cultured in serum-free medium, which lacks phosphatases required to convert tedizolid to its active form (*37*). We found that combination treatment preferentially depleted the LSC-enriched CD34$^+$ fraction to a greater extent than treatment with either drug alone (Fig. 2E, top two rows, and fig. S3B). The same combination treatment did not selectively deplete the CD34$^+$ fraction in cord blood samples, which is enriched for normal hematopoietic stem and progenitor cells (HSPCs) (Fig. 2E, bottom row, and fig. S3B). These data suggest that pharmacologic inhibition of mitochondrial translation sensitizes LSC-enriched populations to venetoclax to a greater degree than non-LSCs and normal HSPCs.

Venetoclax suppresses mitochondrial respiration through inhibition of complex I

To gain genome-wide insights into the mechanisms by which inhibition of mitochondrial translation overcomes venetoclax resistance, we performed RNA sequencing (RNA-seq) of MOLM13-R2 cells treated with venetoclax alone, tedizolid alone, or a combination of the two drugs for 4 days. We performed gene set enrichment analysis (GSEA) on gene expression data of treated samples relative to control samples with the MSigDB v6.2 Hallmark (H) collection. Analysis of tedizolid-treated samples yielded 12 significantly enriched up-regulated gene sets [false discovery rate (FDR) *q* value < 0.25; data file S1]. The top-ranked gene set was oxidative phosphorylation (OXPHOS) (Fig. 3A), likely reflecting a compensatory nuclear transcriptional response to inhibition of mitochondrial respiration by tedizolid. Analysis of venetoclax-treated samples also demonstrated enrichment of the OXPHOS hallmark, which was ranked third among 18 significantly enriched up-regulated gene sets (FDR *q* value < 0.25; Fig. 3A and data file S2), suggestive of a potential impact on OXPHOS activity by venetoclax. Combination treatment similarly resulted in strong enrichment of the OXPHOS gene set (Fig. 3A and data file S3). To further define the impact of drug treatment on OXPHOS, we performed hierarchical clustering and heatmap analysis of the 200 genes

in the OXPHOS hallmark gene set. This analysis revealed that venetoclax treatment up-regulated the expression of most genes in the OXPHOS gene set and induced a transcriptional response profile that was distinct from those of tedizolid and combination treatment (Fig. 3B and data file S4).

On the basis of the above findings, we hypothesized that venetoclax treatment could affect mitochondrial structure and function even in highly resistant cells. To test this hypothesis, we first examined the effect of drug treatment on the mitochondrial ultrastructure in MOLM13-R2 cells using transmission electron microscopy. Treatment with tedizolid alone caused a loss of cristae structure (Fig. 3C, bottom left), which is associated with mitochondrial dysfunction (*38*). We also observed an increase in mitochondrial area and length, suggestive of increased mitochondrial fusion in response to mitochondrial stress (Fig. 3, D and E) (*39*). These findings are consistent with the requirement for mitochondrial protein synthesis to maintain mitochondrial structural integrity (*40, 41*). We observed similar alterations in mitochondrial ultrastructure with single-agent venetoclax treatment [Fig. 3, C (top right), D, and E], despite no detectable increase in apoptosis at the concentration tested (fig. S1A). The combination of tedizolid and venetoclax further exacerbated these changes, resulting in mitochondrial swelling and the appearance of mitochondrial vacuolization [Fig. 3, C (bottom right), D, and E].

To directly interrogate the effect of drug treatment on mitochondrial bioenergetics, we measured the oxygen consumption rate (OCR) of drug-treated cells using the Seahorse Extracellular Flux Analyzer. MOLM13-R2 cells treated with tedizolid alone for 4 days displayed a substantial reduction in OCR at baseline and after mitochondrial uncoupling with carbonyl cyanide-4-(trifluoromethoxy)phenylhydrazone (FCCP) (Fig. 3F), indicating a defect in electron transport chain (ETC) function. Treatment with venetoclax alone at 500 nM also progressively reduced basal and maximal respiratory capacity in MOLM13-R2 and resistant OCI-AML2 cells (Fig. 3F and fig. S4, A and B). The kinetics of OCR suppression coincided with the kinetics of cell death (Fig. 2C). The addition of venetoclax to tedizolid treatment further decreased mitochondrial respiration capacity (Fig. 3F). To confirm that the reduction in mitochondrial respiration with venetoclax exposure was not simply due to apoptosis induction, we repeated the experiment using 143B osteosarcoma cells, which are highly resistant to the proapoptotic effects of venetoclax (IC$_{50}$, ~10 μM; fig. S4C), and found that venetoclax still reduced the basal and maximal respiratory capacity of 143B cells in a concentration-dependent manner (Fig. 3G).

Because OCR is a surrogate measure of ETC activity, a potential mechanism by which venetoclax suppresses mitochondrial respiration is through inhibition of specific complexes in the ETC. To test this hypothesis, we determined the impact of venetoclax on the enzymatic activity of ETC complexes immunocaptured from bovine heart mitochondria. Venetoclax treatment decreased complex I activity to about 60% of DMSO control activity but had minimal or no effect on the activity of the other complexes (Fig. 3H). Although a dose response was observed in the subnanomolar range, the degree of inhibition plateaued at ~60% at concentrations above 0.5 nM (Fig. 3I). To further assess the effect of venetoclax on complex I activity, we purified the enzyme complex from detergent-solubilized bovine heart mitochondria in two sequential chromatography steps (*42*). The first step by ion exchange chromatography resulted in a partially purified preparation, which was further purified in the second step by gel filtration chromatography to obtain a fully purified preparation of complex I (fig. S4D). Nicotinamide adenine dinucleotide plus

Fig. 3. Venetoclax decreases mitochondrial respiration by inhibiting complex I of the ETC. (**A**) GSEA of RNA-seq data generated from MOLM13-R2 cells treated with DMSO (vehicle), venetoclax alone (500 nM), tedizolid alone (5 µM), or a combination of the two drugs for 4 days. (**B**) Heatmap showing the relative expression of genes in the OXPHOS hallmark gene set in MOLM13-R2 cells treated with the indicated drug(s) relative to DMSO treatment. $n = 2$ technical replicates for each treatment condition. (**C**) Transmission electron microscopy images of MOLM13-R2 cells treated with DMSO (vehicle), venetoclax alone (500 nM), tedizolid alone (5 µM), or a combination of the two drugs for 4 days. Scale bars, 400 nm. (**D** and **E**) Quantification of mitochondrial area (D) and length (E) in MOLM13-R2 cells treated as in (C). A random selection of 30 mitochondria across different fields was analyzed for each condition. (**F**) Oxygen consumption rates (OCRs) in MOLM13-R2 after treatment with DMSO (vehicle), venetoclax (500 nM), tedizolid (5 µM), or a combination of the two drugs for 3 days. OCR was measured after successive injections of oligomycin (oligo), FCCP, and rotenone/antimycin A (Rot/AA). $n = 6$ to 10 technical replicates. (**G**) OCRs in 143B cells after treatment with DMSO (vehicle) or venetoclax at the indicated concentration for 3 days. $n = 6$ to 10 technical replicates. (**H**) Enzymatic activity of the indicated ETC complex immunocaptured from bovine heart mitochondria in the presence of DMSO (vehicle) or venetoclax (500 nM for complex I and 2 µM for complex II, III, IV, and V). $n = 3$ technical replicates. (**I**) Enzymatic activity of complex I immunocaptured from bovine heart mitochondria in the presence of varying concentrations of venetoclax. $n = 3$ technical replicates. (**J**) BN-PAGE analysis of complex I, II, III, IV, and V expression in mitochondria isolated from MOLM13-R2 cells treated with DMSO (vehicle) or venetoclax (500 nM) for 4 days. Representative data of $n = 3$ biological replicates. (**K**) Maximal OCRs in MOLM13-R2 and 143B cells transduced with an empty (EV) or *NDI1*-expressing lentiviral vector after treatment with DMSO (vehicle) or venetoclax (500 nM). $n = 3$ to 10 technical replicates. Data shown are means ± SEM. Statistical significance was determined by ANOVA. *$P \leq 0.05$. NS, not significant.
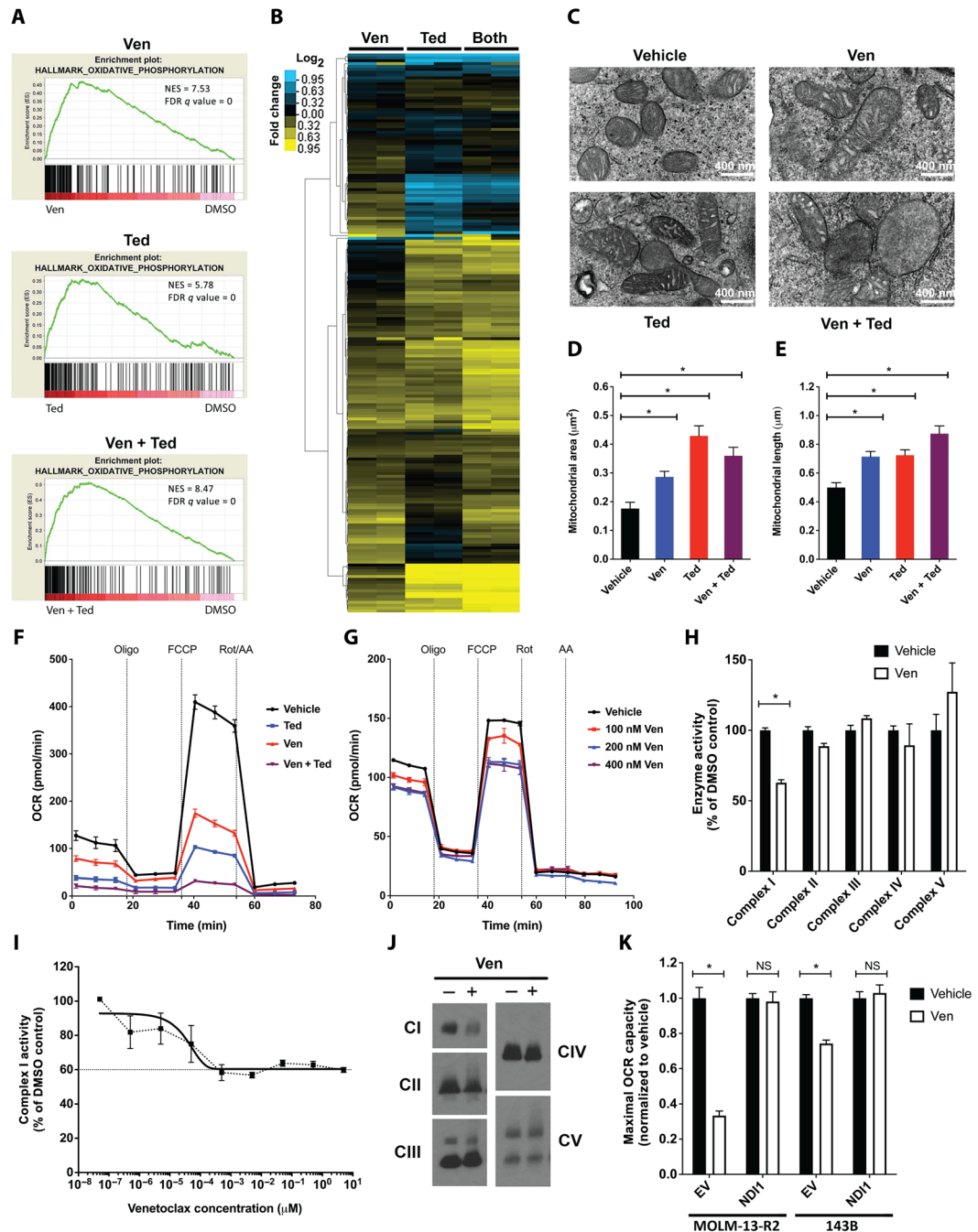
hydrogen dehydrogenase (NADH) activity was measured after each purification step in a spectrophotometric assay (*43*). Consistent with our findings with immunocaptured complex I, venetoclax treatment at 5 µM decreased the activity of partially purified complex I (fig. S4E). However, fully purified complex I was not inhibited by venetoclax at the same concentration (fig. S4E). This finding suggests that the inhibition of complex I by venetoclax relies on a protein or cofactor that can be removed during protein purification.

Given that ETC activity has previously been linked to the assembly and stability of ETC complexes (*44*, *45*), we determined the quantity of assembled complexes by blue native polyacrylamide gel electrophoresis (BN-PAGE) analysis of mitochondrial lysates. Treatment of MOLM13-R2 cells with venetoclax at 400 nM for 3 days specifically reduced the quantity of assembled complex I but not the other complexes (Fig. 3J). To confirm that the observed defect in mitochondrial respiration was due to reduced complex I activity, we leveraged

Sharon *et al.*, *Sci. Transl. Med.* **11**, eaax2863 (2019)   30 October 2019

6 of 15

the ability of the single subunit yeast NADH dehydrogenase (NDI1 protein) to complement mammalian complex I activity (*46*). Expression of *NDI1* completely rescued MOLM13-R2 and 143B cells from the suppressive effects of venetoclax on maximal respiratory capacity (Fig. 3K). Together, our results demonstrate that venetoclax has an inhibitory activity against complex I that is independent of its proapoptotic effects.

ISR activation overcomes venetoclax resistance

Mammalian cells respond to mitochondrial stressors including ETC and mitochondrial translation inhibitors by activating an evolutionarily conserved homeostatic program known as the integrated stress response (ISR) (*47*). A key regulator of ISR signaling is the α-subunit of eukaryotic translation initiation factor 2 (eIF2α) (*48*). Phosphorylation of eIF2α at serine-51 by direct upstream kinases, including protein kinase R (PKR)–like endoplasmic reticulum kinase (PERK) general control nonderepressible 2, heme-regulated inhibitor, and PKR, causes global inhibition of protein synthesis but concurrently up-regulates the translation of specific mRNA transcripts of stress response genes including activating transcription factor 4 (*ATF4*). ATF4 is a transcription factor that promotes the expression of other stress response genes such as C/EBP homologous protein (*CHOP*). This coordinated response attempts to restore cellular homeostasis, but excessive and/or prolonged ISR activation eventually causes cell death through a variety of mechanisms (*48*).

On the basis of our findings demonstrating a negative impact of venetoclax and tedizolid on mitochondrial function, we hypothesized that venetoclax and tedizolid can individually trigger a sublethal ISR, and the combination would activate a more intense ISR that ultimately results in cell death. To test this hypothesis, we first monitored the effects of venetoclax and tedizolid on ISR activation in MOLM13-R2 cells. In line with our hypothesis, single-agent treatment with venetoclax or tedizolid increased the phosphorylation of eIF2α at S51, which was further increased by combination treatment (Fig. 4A). We also tested rotenone, a prototypic complex I inhibitor, in place of venetoclax and observed a similar pattern of up-regulation in eIF2α phosphorylation (fig. S5A).

To assess the effects on downstream ISR signaling, we generated an ATF4 reporter cell line that constitutively expressed a chimeric transcript composed of the 5′ end of *ATF4* fused in frame to the coding sequence of *GFP* (*49*). The intensity of GFP fluorescence thus served as a monitor of translation efficiency of the *ATF4* transcript. Similar to our findings with eIF2α phosphorylation, each drug alone induced modest expression of the reporter transcript, but the combination resulted in the highest intensity (Fig. 4B). These results were confirmed by intracellular flow cytometry analysis of endogenous ATF4 protein expression (fig. S5B). To determine whether downstream ISR transcriptional programs were affected, we generated a second reporter cell line that expressed GFP under control of the *CHOP* promoter, which is transcriptionally activated by ATF4 (*50*). Expression of the GFP reporter was again highest with combination treatment compared to treatment with single agents (Fig. 4C).

To determine whether ISR activation is necessary for overcoming resistance, we used a chemical inhibitor of ISR, known as ISRIB, to block the downstream effects of eIF2α phosphorylation (*51*, *52*). Exposure to ISRIB effectively suppressed the increase in GFP expression after drug treatment in the ATF4 and CHOP reporter cell lines (Fig. 4, D and E), confirming its ability to block downstream ISR signaling in our system. Treatment with ISRIB rescued the viability of MOLM13-R2 cells treated with tedizolid and venetoclax (Fig. 4F), demonstrating

a requirement for ISR activation in mediating this effect. ISRIB also rescued the viability of two primary human AML samples treated with venetoclax and doxycycline in vitro (fig. S5, C and D).

Next, we queried whether direct ISR activation is sufficient to resensitize resistant AML cells to venetoclax. To address this issue, we used three small-molecule compounds that activate ISR signaling in different ways: CCT020312, which selectively and potently activates PERK independently of endoplasmic reticulum (ER) stress (*53*); DHBDC [3-(2,3-dihydrobenzo[b][1,4]dioxin-6-yl)-5,7-dihydroxy-4H-chromen-4-one], which is a specific dual activator of PKR and PERK (*54*); and salubrinal, which prevents the dephosphorylation of eIF2α by selectively inhibiting its phosphatases including growth arrest and DNA damage–inducible 34 (GADD34) (*55*). Treatment with each compound was sufficient to restore venetoclax sensitivity in MOLM13-R2 cells (Fig. 4G and fig. S5, E and F). The addition of ISRIB to cells treated with CCT020312 and venetoclax suppressed ISR activation as monitored by ATF4 reporter expression and rescued the cells from death, ruling out the possibility of an off-target effect of CCT020312 (Fig. 4G and fig. S5G). Overall, these findings demonstrate that venetoclax and protein synthesis inhibitor antibiotics cooperate to activate a heightened ISR that in turn causes cell death.

Combination treatment does not affect BCL-2 family members

Combination treatment with tedizolid and venetoclax activated the intrinsic apoptotic pathway as evidenced by cytochrome C release (fig. S6A), caspase 3/7 activation (fig. S6B), and annexin V binding to phosphatidylserine on the surface of apoptotic cells (Fig. 2C). A possible explanation for the induction of intrinsic apoptosis after ISR activation is a shift in the balance between antiapoptotic and proapoptotic proteins in the BCL-2 family. Previous studies have shown that ISR signaling can up-regulate the expression of proapoptotic proteins such as BIM (*56*) and reduce the expression of antiapoptotic proteins such as MCL-1 (*57*), thereby priming cells to undergo apoptosis. To test this hypothesis, we measured the expression of a panel of antiapoptotic and proapoptotic proteins in MOLM13-R2 cells after treatment with venetoclax alone, tedizolid alone, or the combination for 3 days, before the onset of extensive cell death on day 4. Treatment with tedizolid alone or the combination did not substantially increase the expression of proapoptotic proteins, including BIM, P53 up-regulated modulator of apoptosis, BAX, and BAK, or decrease the expression of antiapoptotic proteins, including BCL-2, MCL-1, and BCL-X$_L$, compared with vehicle (fig. S6C). Blockade of ISR signaling with the addition of ISRIB failed to alter the expression of BCL-2, MCL-1, and BIM (fig. S6D). Tedizolid treatment also did not interfere with the binding between MCL-1 and BIM (fig. S6E). To further assess the role of BIM, we generated *BIM* knockout MOLM13-R2 cells using CRISPR-Cas9 (fig. S6F) and found that the knockout cells remained sensitive to the combination of tedizolid and venetoclax (fig. S6G). On the basis of these results, we postulated that other mechanisms independent of changes in the expression or function of BCL-2 family members are involved.

ISR activation triggers cell death through suppression of glycolytic capacity

An important clue to the mechanism surfaced when we determined the impact of ISRIB on the glycolytic and mitochondrial respiratory capacity of drug-treated cells by measuring their extracellular acidification rate (ECAR) and OCR, respectively. As presented above,
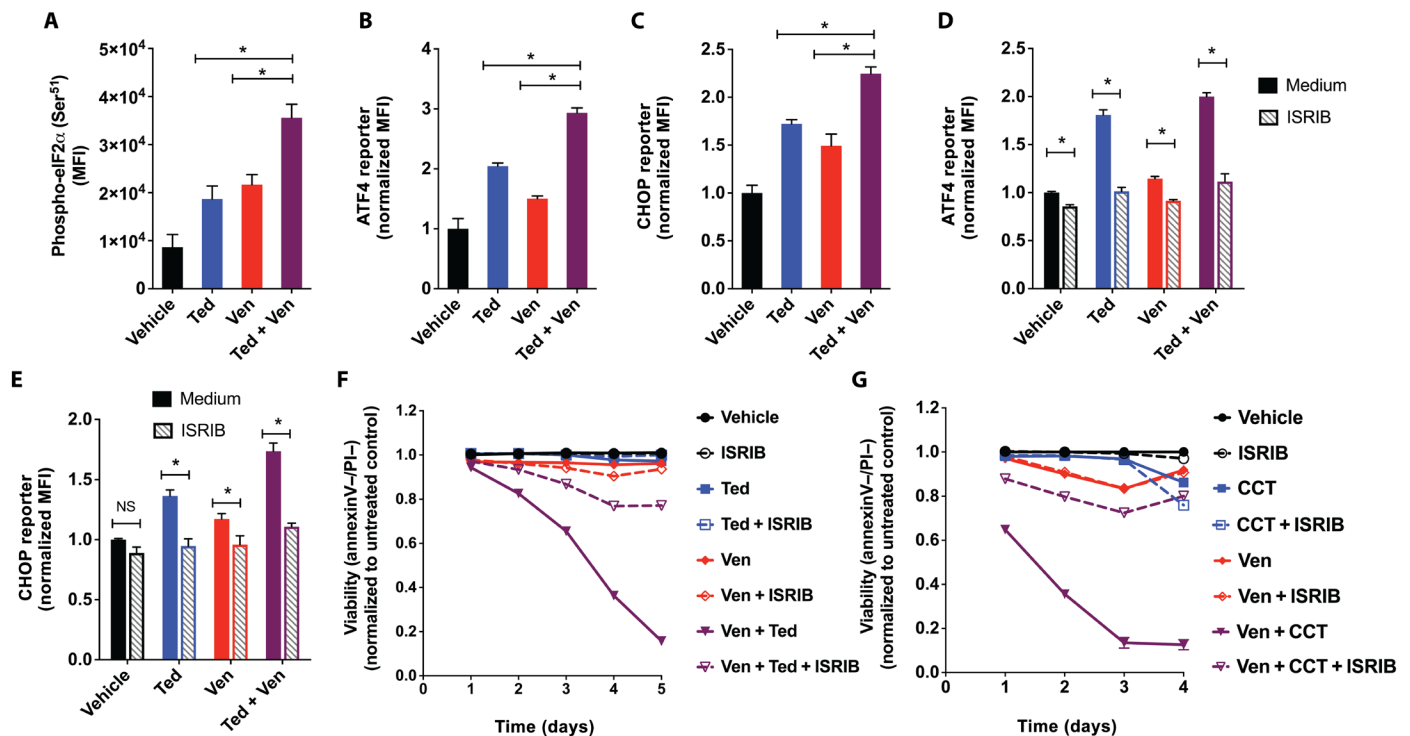
Fig. 4. Venetoclax and tedizolid cooperate to activate a heightened ISR, which is required for the induction of cell death. (**A**) Phosphorylation of eIF2α at serine-51 as determined by intracellular flow cytometry in MOLM13-R2 cells after treatment with DMSO (vehicle), tedizolid (5 μM), venetoclax (500 nM), or a combination of the two drugs for 2 days. $n = 3$ technical replicates. MFI denotes mean fluorescent intensity. (**B** and **C**) Relative intensity of GFP expression in MOLM13-R2 cells engineered to express an ATF4 (B) or CHOP (C) reporter construct after treatment with DMSO (vehicle), tedizolid (5 μM), venetoclax (500 nM), or a combination of the two drugs for 2 days. $n = 3$ technical replicates. (**D** and **E**) Relative intensity of GFP fluorescence in MOLM13-R2 cells engineered to express an ATF4 (D) or CHOP (E) reporter construct after treatment with DMSO (vehicle), tedizolid (5 μM), venetoclax (500 nM), or a combination of the two drugs for 2 days in the absence or presence of ISRIB (1 μM). $n = 3$ technical replicates. (**F**) Viability of MOLM13-R2 cells after treatment with DMSO (vehicle), venetoclax (500 nM), tedizolid (5 μM), or a combination of the two drugs in the absence or presence of ISRIB (1 μM) over the course of 5 days. $n = 3$ technical replicates. (**G**) Viability of MOLM13-R2 cells after treatment with DMSO (vehicle), venetoclax (500 nM), CCT020312 (CCT, 2 μM), or a combination of the two drugs in the absence or presence of ISRIB (1 μM) over the course of 4 days. $n = 3$ technical replicates. Data shown are means ± SEM. Statistical significance was determined by ANOVA. *$P \leq 0.05$. NS, not significant.

treatment with tedizolid + venetoclax substantially suppressed mitochondrial respiration (Fig. 3F). Despite their low OXPHOS activity, cells treated with CCT020312 or tedizolid in combination with venetoclax had less glycolytic capacity than cells treated with vehicle or single agents (Fig. 5, A and B). ISRIB was able to restore the glycolytic capacity of combination-treated cells to that of cells treated with single agents. This effect was specific for glycolytic activity because ISRIB was unable to rescue the defect in mitochondrial respiration in cells treated with tedizolid + venetoclax (fig. S7A). The inability to maintain glycolysis during OXPHOS inhibition would be predicted to result in an energetic crisis that causes cell death. The intracellular ATP concentration of cells treated with venetoclax + tedizolid for 3 days (only before the onset of extensive cell death) was only ~20% of that in untreated cells and lower than the concentrations in cells treated with individual drugs (Fig. 5C). ISRIB treatment increased the ATP concentration in combination-treated cells to that of cells treated with tedizolid alone, likely due to increased ATP generation from glycolysis (Fig. 5C). To show that the rescue by ISRIB was dependent on glycolysis, we switched the carbon source in the culture medium from glucose to galactose. Cells grown in galactose-containing medium are forced to rely on OXPHOS for ATP production because glycolytic metabolism of galactose alone yields no net ATP. In line with our hypothesis, ISRIB treatment failed to

rescue cells treated with venetoclax in combination with CCT020312 or tedizolid in galactose-containing medium (Fig. 5D and fig. S7B). Overall, these findings indicate that the heightened ISR activation induced by combination treatment compromises the capacity of cells to use glycolysis to maintain ATP concentration during OXPHOS inhibition, which, in turn, causes an energetic crisis and eventual cell death through induction of apoptosis (*58*).

Combination of tedizolid and venetoclax demonstrates antileukemic activity in vivo

As an initial investigation into the efficacy of tedizolid and venetoclax in vivo, we transplanted 1×10^5 MOLM13-R2 cells by tail vein injection into nonobese diabetic (NOD)/severe combined immunodeficient (SCID)/*Il2rg*$^{-/-}$ (NSG) mice without conditioning. Five days after transplantation, the mice were randomized to receive treatment with vehicle, venetoclax alone (100 mg/kg per day by oral administration), tedizolid alone (30 mg/kg per day by oral administration), or a combination of the two drugs for 17 consecutive days. The drugs were administered at clinically relevant doses on the basis of the results of prior studies in mice and humans (*5, 9, 30, 59, 60*). At the end of the treatment period, cells from the BM and spleen were collected and analyzed for leukemic burden by flow cytometry. Leukemic burden was lowest in the cohort of mice treated with
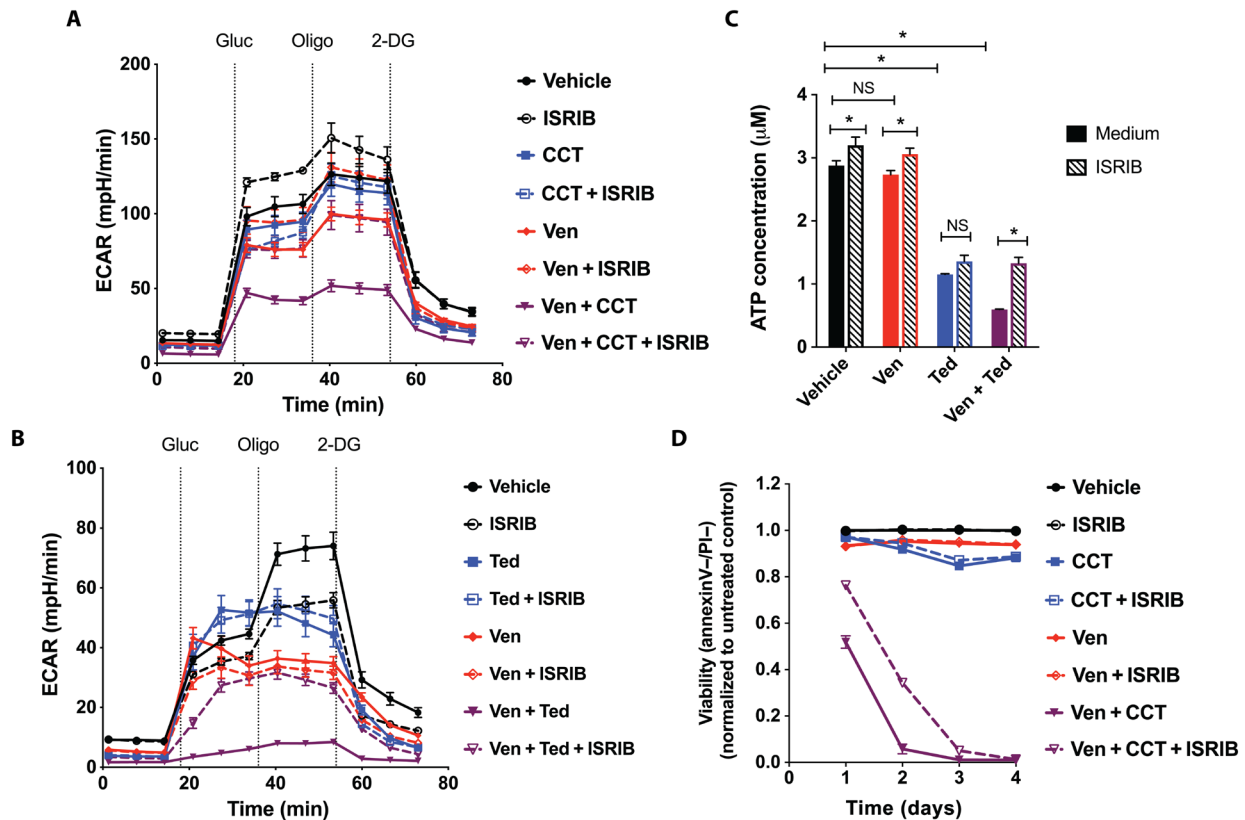
Fig. 5. ISR activation promotes cell death through inhibition of glycolytic capacity. (**A**) Extracellular acidification rates (ECARs) in MOLM13-R2 cells after treatment with DMSO (vehicle), CCT020312 (CCT, 2 μM), venetoclax (500 nM), or a combination of the two drugs in the absence or presence of ISRIB (1 μM) for 2 days. ECAR was measured after sequential injections of glucose (Gluc), oligomycin (Oligo), and 2-deoxyglucose (2-DG). $n = 6$ to 8 technical replicates. (**B**) ECARs in MOLM13-R2 cells after treatment with DMSO (vehicle), tedizolid (5 μM), venetoclax (500 nM), or a combination of the two drugs in the absence or presence of ISRIB (1 μM) for 3 days. $n = 6$ to 8 technical replicates. (**C**) Intracellular ATP concentrations in MOLM13-R2 cells after treatment with DMSO (vehicle), tedizolid (5 μM), venetoclax (500 nM), or a combination of the two drugs in the absence or presence of ISRIB (1 μM) for 3 days. $n = 3$ technical replicates. (**D**) Viability of MOLM13-R2 cells in glucose-free/galactose-containing growth medium after treatment with DMSO (vehicle), CCT020312 (CCT, 2 μM), venetoclax (500 nM), or a combination of the two drugs in the absence or presence of ISRIB (1 μM) over the course of 4 days. $n = 3$ technical replicates. Data shown are means ± SEM. Statistical significance was determined by ANOVA. *$P \le 0.05$. NS, not significant.

venetoclax + tedizolid compared with treatment with vehicle or single agents (Fig. 6A).

To determine the efficacy of combination treatment in mice with established disease, we generated a primary AML sample with acquired resistance by treating NSG mice engrafted with a sensitive sample (SU048) with venetoclax (100 mg/kg per day by oral administration) continuously until disease progression, which took about 4 weeks. We collected the resulting resistant cells (SU048-R) from the BM and transplanted them (1×10^5 cells per mouse) by tail vein injection into sublethally irradiated (2.5 gray) NSG recipients. Five weeks after transplantation, BM cells were collected by femoral aspiration and analyzed for leukemic engraftment before treatment. After confirmation of engraftment, the mice were randomized to receive treatment with vehicle, venetoclax alone (100 mg/kg per day by oral administration), tedizolid alone (10 mg/kg twice daily by intraperitoneal injection), or a combination of the two drugs for 20 days on a 5-days-on, 2-days-off schedule. The route of tedizolid administration was switched from oral to intraperitoneal to improve tolerability of combination treatment by minimizing the frequency of oral gavages. Leukemic burden in the BM and spleen at the end of treatment was lowest in the combination treatment arm compared with the remaining arms (Fig. 6B and fig. S8A). The treatment with

venetoclax + tedizolid reduced leukemic burden from pretreatment values in the BM (Fig. 6B and fig. S8A). To determine whether LSCs were targeted, we collected splenocytes from these animals at the end of treatment and transplanted equivalent numbers (5×10^4) of cells by tail vein injection into sublethally irradiated secondary NSG recipients. Leukemic engraftment in the BM of secondary recipients was determined 5 weeks after transplantation. Cells collected from animals treated with venetoclax + tedizolid had less secondary engraftment potential than cells from the other treatment arms (Fig. 6C).

To further investigate the treatment efficacy of venetoclax + tedizolid in vivo, we transplanted 2×10^5 to 4×10^5 cells from two primary AML samples (120860 and 151044) into sublethally irradiated NSG mice. The samples were T cell–depleted before transplantation to enhance engraftment in NSG mice (*61*). Eight to 16 weeks after transplantation, we measured leukemic engraftment in the BM before treatment initiation. After confirmation of engraftment, the mice were randomized to one of the four treatment arms as described above. Treatments were administered on a 5-days-on, 2-days-off schedule. The duration of treatment was 8 days for mice engrafted with 120860 and 29 days for 151044. At the end of treatment, leukemic burden in the BM and/or spleen was determined. For both patient-derived xenograft (PDX) models, treatment with venetoclax + tedizolid resulted
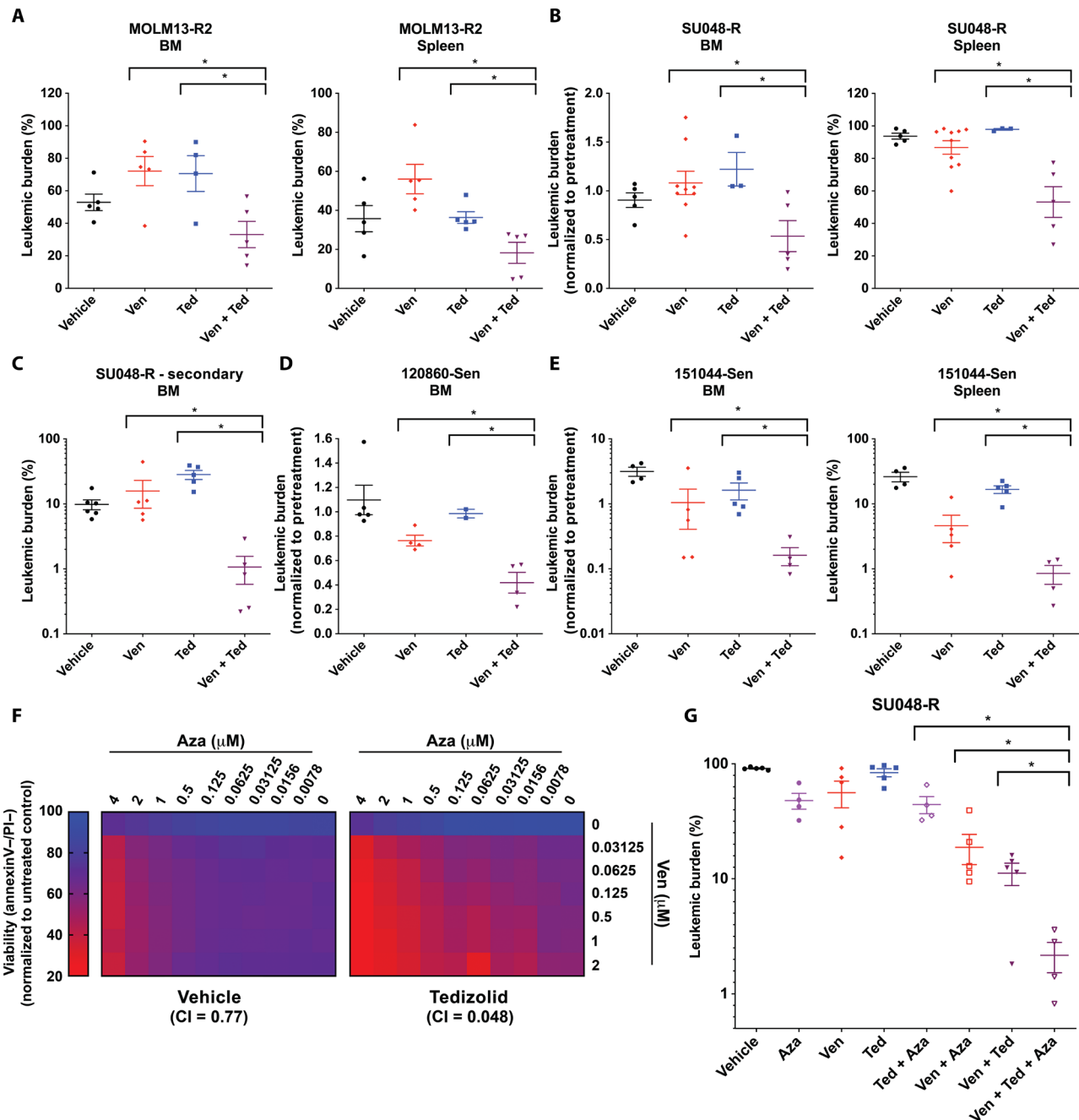
Sharon *et al.*, *Sci. Transl. Med.* **11**, eaax2863 (2019)   30 October 2019

9 of 15

Fig. 6. Tedizolid treatment enhances the antileukemic activity of venetoclax in vivo. (**A**) Leukemic burden in bone marrow (BM) and spleen of NSG mice transplanted with MOLM13-R2 cells after treatment with vehicle, venetoclax alone, tedizolid alone, or a combination of the two drugs for 17 consecutive days. (**B**) Leukemic burden in BM and spleen of NSG mice transplanted with a venetoclax-resistant AML sample (SU048-R) after treatment with vehicle, venetoclax alone, tedizolid alone, or a combination of the two drugs for 20 days on a 5-days-on, 2-days-off schedule. BM engraftment was confirmed before starting treatment. BM leukemic burden data shown are normalized to the pretreatment value for each animal. Values less than 1 are indicative of a reduction in burden from before treatment. (**C**) Leukemic engraftment in the BM of NSG mice at 5 weeks after secondary transplantation of spleen cells collected from animals treated in (B). (**D**) Leukemic burden in BM of NSG mice transplanted with a primary human AML sample (120860) after treatment with vehicle, venetoclax alone, tedizolid alone, or a combination of the two drugs for 8 days on a 5-days-on, 2-days-off schedule. BM engraftment was confirmed before starting treatment. BM leukemic burden data shown are normalized to the pretreatment value for each animal. Values less than 1 are indicative of a reduction in burden from before treatment. (**E**) Leukemic burden in BM and spleen of NSG mice transplanted with a primary AML sample (151044) after treatment with vehicle, venetoclax alone, tedizolid alone, or a combination of the two drugs for 29 days on a 5-days-on, 2-days-off schedule. BM engraftment was confirmed before starting treatment. BM leukemic burden data shown are normalized to the pretreatment value for each animal. Values less than 1 are indicative of a reduction in burden from before treatment. (**F**) Heatmap showing the viability of MOLM13-R2 cells treated with serial dilutions of azacitidine and venetoclax in the absence or presence of tedizolid (5 μM). Combination index (CI) was determined by the CalcuSyn software. (**G**) Leukemic burden in the spleen of NSG mice transplanted with SU048-R after treatment with the indicated drugs or drug combinations for 24 days on a 5-days-on, 2-days-off schedule. BM engraftment was confirmed before starting treatment. Data shown are means ± SEM. Statistical significance was determined by ANOVA. *$P \leq 0.05$. All individual animal data are reported in data file S5.

Sharon *et al.*, *Sci. Transl. Med.* **11**, eaax2863 (2019)   30 October 2019

10 of 15

in a greater reduction in leukemic burden from pretreatment values compared with the other treatment arms (Fig. 6, D and E, and fig. S8, B and C).

To determine whether the addition of tedizolid can enhance the activity of venetoclax in combination with azacitidine, we performed experiments involving the combination of all three drugs. The addition of tedizolid enhanced the synergy between venetoclax and azacitidine in killing MOLM13-R2 cells in vitro (Fig. 6F). To evaluate the efficacy of the triplet combination in vivo, we transplanted SU048-R cells (1×10^5 cells per mouse) into sublethally irradiated NSG mice and confirmed BM engraftment 5 weeks after transplantation. The engrafted animals were then randomized to receive treatment with vehicle, each drug alone (venetoclax, 100 mg/kg per day by oral administration; tedizolid, 10 mg/kg twice daily by intraperitoneal injection; azacitidine, 0.5 mg/kg per day by intraperitoneal injection), three different doublet combinations, or the triplet combination for 24 days on a 5-days-on, 2-days-off schedule. Consistent with the in vitro studies, leukemic burden was lowest in the triplet combination treatment arm compared with all the remaining arms at completion of treatment (Fig. 6G). There was no overt evidence of toxicity associated with triplet combination therapy (fig. S9, A to C). Overall, the animal studies demonstrate that the combination of tedizolid and venetoclax is more active than single-agent treatments against both venetoclax-resistant and sensitive AML and cooperates with azacitidine to enhance killing of AML cells.

DISCUSSION

Venetoclax in combination with HMAs or LDAC is approved for the treatment of newly diagnosed patients with AML who are not eligible for intensive chemotherapy. Although these combination regimens are anticipated to transform the treatment of patients with AML, about 30 to 40% of treatment-naïve patients (20, 21, 62) and even a higher proportion of relapsed/refractory patients are primary nonresponders (22). Moreover, most responders eventually experience disease progression (20, 21, 62). Hence, the development of alternative doublet combinations or triplet combinations that build upon this backbone is required to improve the clinical efficacy of venetoclax. In this study, we addressed this need by performing an unbiased genome-wide CRISPR knockout screen to discover genes that, upon inactivation, overcome venetoclax resistance. The screen led us to identify multiple genes that encode components of the mitochondrial translational machinery. This finding has immediate clinical relevance because a number of FDA-approved antibiotics have well-characterized inhibitory properties against mitochondrial translation. Our current study focused on doxycycline and tedizolid. Tedizolid is a second-generation oxazolidinone-class antibiotic that blocks mitochondrial protein synthesis at clinically relevant concentrations and with greater potency than linezolid, a first-generation oxazolidinone (30, 63). Tedizolid is approved for the treatment of acute bacterial skin and skin structure infections caused by Gram-positive bacteria (64). Our experiments showed that although tedizolid as a single agent had no or limited antileukemic activity, it effectively restored venetoclax sensitivity across a panel of AML cell lines with intrinsic or acquired resistance in vitro and enhanced the antileukemic activity of venetoclax in PDX models of AML.

Inhibition of mitochondrial translation as a strategy to enhance venetoclax activity has previously been described. We initially reported that treatment with tigecycline enhanced sensitivity to venetoclax in

AML cells (9). More recently, Ravà et al (65). confirmed this finding in a preclinical model of *MYC/BCL2* double-hit B cell lymphoma. However, neither study investigated the mechanism of synergy between mitochondrial translation inhibitors and venetoclax. The present study delineated the mechanism and, in the process, discovered that ISR activation plays a critical role in mediating the synergistic effect and that venetoclax has inhibitory activity against complex I of the ETC.

Several studies previously reported a reduction in mitochondrial respiration after exposure to BH3 mimetics including venetoclax. Lagadinou et al. showed that treatment with ABT-263 [a BH3 mimetic that targets BCL-2, BCL-X$_L$, and BCL-2–like protein 2 (BCL2L2, also known as BCL-W)] decreased OXPHOS in primary AML cells (66). Subsequent reports showed that treatment with venetoclax also disrupted mitochondrial respiration in other cancer cell types (67, 68). However, the mechanism by which venetoclax and other BH3 mimetics mediated this effect was unknown. In this study, we observed that venetoclax treatment up-regulated the expression of OXPHOS genes, disrupted mitochondrial ultrastructure, and reduced OXPHOS. Using a combination of biochemical and genetic approaches, we localized the defect to complex I of the ETC. Expression of the yeast *NDI1*, which serves to bypass complex I defects (46), completely rescued the inhibition of OXPHOS by venetoclax treatment, providing strong evidence for complex I as the main target of inhibition. Pollyea et al. (69) recently reported that treatment with venetoclax + azacitidine suppressed complex II activity, which was attributed to a reduction in SDHA glutathionylation. However, their study did not report the impact of venetoclax + azacitidine on other ETC complexes, including complex I. Our experiments demonstrated only a minimal reduction in complex II activity and no changes in total SDHA expression, although we only studied the effects of venetoclax as a single agent. Thus, there were substantial differences in assay methodologies and treatment conditions that preclude a direct comparison of the two studies. Nevertheless, we speculate that the abovementioned effects on complex I and II can occur concurrently, contributing to the disruption of energy metabolism in treated cells.

ISR is an evolutionarily conserved cytoprotective response that is activated by a variety of stressors including mitochondrial stress (47). Here, we showed that treatment with venetoclax alone activated ISR, consistent with its inhibitory activity on complex I. Venetoclax cooperated with tedizolid to achieve synergistic ISR activation, which was necessary for the induction of cell death. A number of pathways downstream of ISR have previously been shown to mediate cell death (48). One such mechanism is the up-regulation of BIM (56), and another is the reduction in MCL-1 expression (57); both can potentially augment sensitivity to venetoclax. However, we detected no substantial changes in the expression of BIM, MCL-1, or other BCL-2 family members. Furthermore, we did not observe a decrease in binding between MCL-1 and BIM with tedizolid treatment. The lack of MCL-1 suppression indicates that the mechanism by which tedizolid circumvents venetoclax resistance is distinct from that of other drugs including TIC10/ONC201 (70), MEK inhibitors (14, 15, 71), and MDM2 inhibitors (14), which decrease MCL-1 protein expression and/or activity. Given the importance of MCL-1 in maintaining survival of normal tissues, we speculate that tedizolid + venetoclax may have a more favorable therapeutic window than other combination regimens.

We found that ISR activation repressed the glycolytic capacity of combination-treated cells despite an almost complete inhibition of OXPHOS activity, rather than acting through changes in the expression

of BCL-2 members. This response was observed only when a strong ISR was activated with combination treatment; cells treated with each drug alone were still able to maintain glycolysis for ATP generation. This inability to increase or maintain glycolytic activity after inhibition of mitochondrial respiration is reminiscent of what Lagadinou *et al.* (*66*) observed in reactive oxygen species (ROS)–low LSCs after treatment with ABT-263. Furthermore, van Galen *et al.* (*72*) showed that ISR activity is higher in LSCs due to the scarcity of eIF2. Together, these findings suggest that LSCs have less glycolytic capacity compared with non-LSCs due to higher ISR activation. This reasoning provides a plausible explanation for why LSCs are more sensitive to OXPHOS inhibition than non-LSCs.

There are several limitations to our study that should be taken into consideration. First, it is not known whether tedizolid can be administered at doses high enough to inhibit mitochondrial translation without causing unacceptable toxicities in humans, especially when given in combination with azacitidine and venetoclax. Second, the duration of treatment for animal experiments was relatively short, which limits our ability to assess impact on survival, durability of response, and toxicity. Last, because we tested only a limited number of AML cell lines and primary samples, it is unclear whether the sensitization effect of tedizolid is broadly applicable to all AML subtypes or restricted to only certain subtypes of AML.

Venetoclax in combination with HMAs has emerged as a potentially transformative therapy for AML. The superior efficacy of this combination appears to be due to its ability to disrupt energy metabolism through inhibition of ETC and amino acid catabolism (*69*, *73*). In this study, we demonstrated that the addition of tedizolid to venetoclax + azacitidine resulted in further enhancement of its antileukemic activity against resistant AML cells in vitro and in vivo. This is presumably due to a greater suppression in OXPHOS and concurrent reduction in glycolytic capacity as a consequence of ISR hyperactivation. Together, we propose that the triplet combination would simultaneously target multiple pathways of energy metabolism, resulting in a complete energetic collapse and subsequent death of resistant AML cells. Our data provide a rational basis for testing the safety and efficacy of this triplet combination in clinical trials.

MATERIALS AND METHODS
Study design
Our overall objective was to develop a strategy to overcome resistance to venetoclax. We performed a genome-wide CRISPR screen to identify genes that, upon inactivation, restored sensitivity to venetoclax in a resistant AML cell line. We used genetic and pharmacologic tools to determine the mechanisms by which inhibition of mitochondrial translation overcomes resistance to venetoclax. We performed in vitro and in vivo experiments to determine whether combination treatment with tedizolid and venetoclax was more effective in killing human AML cells than treatment with single agents. Mice were randomly assigned to the different treatment arms as indicated. Researchers were not blinded to treatment assignment. The primary endpoint was leukemia burden in BM or spleen at the completion of treatment. Sample size was calculated to achieve 80% power with a type I error rate of 5% and an anticipated difference of ~20% in mean leukemia burden values between two arms. The duration of treatment was determined before starting each experiment unless the animals were euthanized because of humane reasons or died

before the end of treatment. All available data points were included in the final analysis.

Ex vivo culture of primary AML cells and cord blood HSPCs
Human AML and cord blood samples were obtained with informed consent according to procedures approved by the University Health Network ethics committee. Primary human AML cells were isolated by differential density centrifugation and cryopreserved in liquid nitrogen. Freshly thawed primary AML cells were grown in X-VIVO 10 medium (Lonza, catalog no. 04-380Q) supplemented with 20% BIT 9500 serum substitute (STEMCELL Technologies, catalog no. 09500) and 2 mM Gluta-Plus, as well as IL-6 (10 ng/ml; PeproTech, catalog no. 200-06), IL-3 (10 ng/ml; PeproTech, catalog no. 200-03), stem cell factor (50 ng/ml; Peprotech, catalog no. 300-07), FLT3-Ligand (50 ng/ml; PeproTech, catalog no. 300-19), granulocyte colony-stimulating factor (10 ng/ml; PeproTech, catalog no. 300-23), and TPO (25 ng/ml; PeproTech, catalog no. 300-18). Genetic characteristics of the primary AML samples used in this study are summarized in table S2. Human HSPCs in cord blood samples were enriched by differential density centrifugation followed by positive enrichment of CD34$^+$ cells using anti-CD34 microbeads (Miltenyi Biotec, catalog no. 130-100-453) as per the manufacturer's protocol. CD34$^+$-enriched cord blood cells were cultured in the same supplemented X-VIVO 10 medium as above for primary AML cells.

Flow cytometric analysis of primary AML samples and cord blood HPSCs in culture
For the detection of CD34 and CD38 expression, cells were pelleted, washed in FACS buffer [1% (v/v) fetal bovine serum in phosphate-buffered saline (PBS)], and stained with the following primary antibodies: allophycocyanin (APC) anti-human CD34 (clone 8G12; BD Biosciences, catalog no. 340441) at a dilution of 1:100 and PE anti-human CD38 (clone HB7; Thermo Fisher Scientific, catalog no. 12-0388-42) at a dilution of 1:100 for 30 min at 4°C. Cells were then washed in FACS buffer and resuspended in 1× annexin binding buffer (Thermo Fisher Scientific, catalog no. V13246) containing fluorescein isothiocyanate (FITC)–conjugated annexin V (Thermo Fisher Scientific, catalog no. A13199) at a dilution of 1:200. Cells were incubated at room temperature in the dark for 15 min before analysis on a BD Accuri C6 flow cytometer.

NSG xenotransplantation
All animal studies were carried out according to the regulations of the Canadian Council on Animal Care and with the approval of the University Health Network Ethics Review Board. Six- to 12-week-old NOD/SCID/*Il2rg*$^{-/-}$ (NSG) mice were bred in-house and used as hosts for xenotransplantation experiments. Both female and male mice were used. MOLM13-R2 and SU048-R AML cells were washed, resuspended in PBS, and transplanted into NSG mice by tail vein injection. Freshly thawed primary AML samples (151044 and 120860) were subjected to T cell depletion using anti-CD3 magnetic beads (Miltenyi Biotec, catalog no. 130-050-101) before transplantation. Unless otherwise indicated, NSG mice were conditioned with 2.5 gray of irradiation.

Drug treatment
With the exception of the MOLM13-R2 model, drug treatment was started after confirmation of AML engraftment in BM. Venetoclax was resuspended in 10% ethanol (Commercial Alcohols, catalog no.

Sharon *et al.*, *Sci. Transl. Med.* **11**, eaax2863 (2019)   30 October 2019

12 of 15

P006EAAN), 30% polyethylene glycol 400 (Sigma, catalog no. 06855-1KG), and 60% PHOSAL 50 PG (Lipoid, catalog no. 368315) at a final concentration of 10 mg/ml. Venetoclax was administered by oral gavage at a dose of 100 mg/kg per day. Tedizolid was administered by either oral gavage or intraperitoneal injection. For oral gavage, tedizolid phosphate tablets (Merck) were crushed and resuspended in 0.9% saline at a concentration of 6 mg/ml (active ingredient) before administration. The oral dose of tedizolid was 30 mg/kg per day. For intraperitoneal injection, tedizolid phosphate (Selleckchem, catalog no. S4641) was dissolved in DMSO at a concentration of 22.5 mg/ml to generate a stock solution. The stock solution was diluted in 0.9% saline to a final concentration of 1 mg/ml immediately before injection. The dose of tedizolid by intraperitoneal injection was 10 mg/kg twice daily. Azacitidine (Cayman Chemical, catalog no. 11164) was dissolved in DMSO at a concentration of 48.84 mg/ml to generate a stock solution. The stock solution was diluted in 0.9% saline to a final concentration of 50 µg/ml immediately before administration. Azacitidine was administered by intraperitoneal injection at a dose of 0.5 mg/kg per day. The duration of treatment was determined before starting each experiment unless the animals were sacrificed due to humane reasons or died before the end of treatment.

Leukemic burden analysis

To confirm leukemic engraftment before drug treatment, BM cells were collected by aspiration of the femur using a 27-gauge needle and analyzed for leukemic burden. After completion of drug treatment, the animals were euthanized, and their BM cells and/or splenocytes were collected for leukemic burden analysis. Cell samples were resuspended in ammonium chloride solution (STEMCELL Technologies, catalog no. 07850) and incubated at room temperature for 5 min to lyse red blood cells. The cells were then washed in FACS buffer and stained with the following fluorophore-conjugated antibodies: PE-Cy7 anti-mouse CD45 (Thermo Fisher Scientific, catalog no. 25-0453-82) at a dilution of 1:100, FITC anti-mouse TER119 (Thermo Fisher Scientific, catalog no. 11-5921-85) at a dilution of 1:100, and APC anti-human CD45 (Thermo Fisher Scientific, catalog no. 17-0459-42) at a dilution of 1:100. The SYTOX Green Dead Cell Stain (Thermo Fisher Scientific, catalog no. S34859) was used to distinguish dead from live cells. The viable human leukemic population was identified as SYTOX Green$^-$, mTER199$^-$, mCD45$^-$, and hCD45$^+$.

Statistics

All data points are represented as means ± SEM. Two-tailed Student's *t* test was used to compare mean values between two groups. One-way or two-way analysis of variance (ANOVA) followed by Dunnett's (one-way) or Sidak (two-way) post hoc testing was used to compare mean values between multiple groups. Statistical analysis was performed using Prism version 6.07 (GraphPad Software, La Jolla, CA). *P* values < 0.05 were considered statistically significant. For GSEA analysis, FDR values < 0.25 were considered statistically significant.

SUPPLEMENTARY MATERIALS

stm.sciencemag.org/cgi/content/full/11/516/eaax2863/DC1
Materials and Methods
Fig. S1. Resistant MOLM13 and MV4-11 cells have higher expression of MCL-1 or BCL-X$_L$.
Fig. S2. Tedizolid treatment suppresses mitochondrial translation and increases sensitivity to pharmacologic inhibition of BCL-2 but not MCL-1 or BCL-X$_L$.
Fig. S3. Doxycycline enhances sensitivity to venetoclax in CD34$^+$ cells from primary AML samples.
Fig. S4. Venetoclax inhibits complex I activity.

Fig. S5. ISR activation is necessary and sufficient to sensitize AML cells to venetoclax.
Fig. S6. Combination treatment with tedizolid and venetoclax does not affect BCL-2 family members.
Fig. S7. ISRIB treatment prevents cell death by promoting glycolysis.
Fig. S8. Tedizolid treatment enhances the anti-leukemic activity of venetoclax in vivo.
Fig. S9. Combination treatment does not cause overt toxicities in PDX models.
Table S1. Engraftment potential of sorted CD34/CD38 fractions from primary AML sample 130578.
Table S2. Genetic characteristics of the primary AML samples and cell lines used in this study.
Data file S1. Gene sets enriched in tedizolid-treated cells.
Data file S2. Gene sets enriched in venetoclax-treated cells.
Data file S3. Gene sets enriched in cells treated with tedizolid and venetoclax.
Data file S4. RNA expression of genes in the OXPHOS gene set normalized to values in DMSO control treated cells.
Data file S5. Individual animal data from in vivo treatment studies.

View/request a protocol for this paper from *Bio-protocol*.

REFERENCES AND NOTES

1. H. Dombret, C. Gardin, An update of current treatments for adult acute myeloid leukemia. *Blood* **127**, 53–61 (2016).
2. F. R. Appelbaum, H. Gundacker, D. R. Head, M. L. Slovak, C. L. Willman, J. E. Godwin, J. E. Anderson, S. H. Petersdorf, Age and acute myeloid leukemia. *Blood* **107**, 3481–3485 (2006).
3. S. P. Glaser, E. F. Lee, E. Trounson, P. Bouillet, A. Wei, W. D. Fairlie, D. J. Izon, J. Zuber, A. R. Rappaport, M. J. Herold, W. S. Alexander, S. W. Lowe, L. Robb, A. Strasser, Anti-apoptotic Mcl-1 is essential for the development and sustained growth of acute myeloid leukemia. *Genes Dev.* **26**, 120–125 (2012).
4. P. Juin, O. Geneste, F. Gautier, S. Depil, M. Campone, Decoding and unlocking the BCL-2 dependency of cancer cells. *Nat. Rev. Cancer* **13**, 455–465 (2013).
5. A. J. Souers, J. D. Leverson, E. R. Boghaert, S. L. Ackler, N. D. Catron, J. Chen, B. D. Dayton, H. Ding, S. H. Enschede, W. J. Fairbrother, D. C. S. Huang, S. G. Hymowitz, S. Jin, S. L. Khaw, P. J. Kovar, L. T. Lam, J. Lee, H. L. Maecker, K. C. Marsh, K. D. Mason, M. J. Mitten, P. M. Nimmer, A. Oleksijew, C. H. Park, C.-M. Park, D. C. Phillips, A. W. Roberts, D. Sampath, J. F. Seymour, M. L. Smith, G. M. Sullivan, S. K. Tahir, C. Tse, M. D. Wendt, Y. Xiao, J. C. Xue, H. Zhang, R. A. Humerickhouse, S. H. Rosenberg, S. W. Elmore, ABT-199, a potent and selective BCL-2 inhibitor, achieves antitumor activity while sparing platelets. *Nat. Med.* **19**, 202–208 (2013).
6. P. D. Bhola, A. Letai, Mitochondria—Judges and executioners of cell death sentences. *Mol. Cell* **61**, 695–704 (2016).
7. R. Pan, L. J. Hogdal, J. M. Benito, D. Bucci, L. Han, G. Borthakur, J. Cortes, D. J. DeAngelo, L. Debose, H. Mu, H. Dohner, V. I. Gaidzik, I. Galinsky, L. S. Golfman, T. Haferlach, K. G. Harutyunyan, J. Hu, J. D. Leverson, G. Marcucci, M. Muschen, R. Newman, E. Park, P. P. Ruvolo, V. Ruvolo, J. Ryan, S. Schindela, P. Zweidler-McKay, R. M. Stone, H. Kantarjian, M. Andreeff, M. Konopleva, A. G. Letai, Selective BCL-2 inhibition by ABT-199 causes on-target cell death in acute myeloid leukemia. *Cancer Discov.* **4**, 362–375 (2014).
8. M. Konopleva, A. Letai, BCL-2 inhibition in AML: An unexpected bonus? *Blood* **132**, 1007–1012 (2018).
9. S. M. Chan, D. Thomas, M. R. Corces-Zimmerman, S. Xavy, S. Rastogi, W.-J. Hong, F. Zhao, B. C. Medeiros, D. A. Tyvoll, R. Majeti, Isocitrate dehydrogenase 1 and 2 mutations induce BCL-2 dependence in acute myeloid leukemia. *Nat. Med.* **21**, 178–184 (2015).
10. M. Konopleva, D. A. Pollyea, J. Potluri, B. Chyla, L. Hogdal, T. Busman, E. McKeegan, A. H. Salem, M. Zhu, J. L. Ricker, W. Blum, C. D. DiNardo, T. Kadia, M. Dunbar, R. Kirby, N. Falotico, J. Leverson, R. Humerickhouse, M. Mabry, R. Stone, H. Kantarjian, A. Letai, Efficacy and biological correlates of response in a phase II study of venetoclax monotherapy in patients with acute myelogenous leukemia. *Cancer Discov.* **6**, 1106–1117 (2016).
11. S. Caenepeel, S. P. Brown, G. Belmontes, G. Moody, K. S. Keegan, D. Chui, D. A. Whittington, X. Huang, L. Poppe, A. C. Cheng, M. Cardozo, J. Houze, Y. Li, B. Lucas, N. A. Paras, X. Wang, J. P. Taygerly, M. Vimolratana, M. Zancanella, L. Zhu, E. Cajulis, T. Osgood, J. Sun, L. Damon, R. K. Egan, P. Greninger, J. McClanaghan, J. Gong, D. Moujalled, G. Pomilio, P. Beltran, C. H. Benes, A. W. Roberts, D. C. Huang, A. Wei, J. Canon, A. Coxon, P. E. Hughes, AMG 176, a selective MCL1 inhibitor, is effective in hematologic cancer models alone and in combination with established therapies. *Cancer Discov.* **8**, 1582–1597 (2018).
12. H. E. Ramsey, M. A. Fischer, T. Lee, A. E. Gorska, M. P. Arrate, L. Fuller, K. L. Boyd, S. A. Strickland, J. Sensintaffar, L. J. Hogdal, G. D. Ayers, E. T. Olejniczak, S. W. Fesik, M. R. Savona, A novel MCL1 inhibitor combined with venetoclax rescues venetoclax-resistant acute myelogenous leukemia. *Cancer Discov.* **8**, 1566–1581 (2018).
13. D. M. Moujalled, G. Pomilio, C. Ghiurau, A. Ivey, J. Salmon, S. Rijal, S. Macraild, L. Zhang, T.-C. Teh, I.-S. Tiong, P. Lan, M. Chanrion, A. Claperon, F. Rocchetti, A. Zichi, L. Kraus-Berthier, Y. Wang, E. Halilovic, E. Morris, F. Colland, D. Segal, D. Huang, A. W. Roberts, A. L. Maragno, G. Lessene, O. Geneste, A. H. Wei, Combining BH3-mimetics to target both

Sharon *et al.*, *Sci. Transl. Med.* **11**, eaax2863 (2019) 30 October 2019

13 of 15

BCL-2 and MCL1 has potent activity in pre-clinical models of acute myeloid leukemia. *Leukemia* **33**, 905–917 (2019).

14. R. Pan, V. Ruvolo, H. Mu, J. D. Leverson, G. Nichols, J. C. Reed, M. Konopleva, M. Andreeff, Synthetic lethality of combined Bcl-2 inhibition and p53 activation in AML: Mechanisms and superior antileukemic efficacy. *Cancer Cell* **32**, 748–760 e6 (2017).

15. M. Konopleva, M. Milella, P. Ruvolo, J. C. Watts, M. R. Ricciardi, B. Korchin, T. McQueen, W. Bornmann, T. Tsao, P. Bergamo, D. H. Mak, W. Chen, J. McCubrey, A. Tafuri, M. Andreeff, MEK inhibition enhances ABT-737-induced leukemia cell apoptosis via prevention of ERK-activated MCL-1 induction and modulation of MCL-1/BIM complex. *Leukemia* **26**, 778–787 (2012).

16. J. T. Opferman, H. Iwasaki, C. C. Ong, H. Suh, S. Mizuno, K. Akashi, S. J. Korsmeyer, Obligate role of anti-apoptotic MCL-1 in the survival of hematopoietic stem cells. *Science* **307**, 1101–1104 (2005).

17. C. J. Campbell, J. B. Lee, M. Levadoux-Martin, T. Wynder, A. Xenocostas, B. Leber, M. Bhatia, The human stem cell hierarchy is defined by a functional dependence on Mcl-1 for self-renewal capacity. *Blood* **116**, 1433–1442 (2010).

18. R. L. Thomas, D. J. Roberts, D. A. Kubli, Y. Lee, M. N. Quinsay, J. B. Owens, K. M. Fischer, M. A. Sussman, S. Miyamoto, Å. B. Gustafsson, Loss of MCL-1 leads to impaired autophagy and rapid development of heart failure. *Genes Dev.* **27**, 1365–1377 (2013).

19. B. Vick, A. Weber, T. Urbanik, T. Maass, A. Teufel, P. H. Krammer, J. T. Opferman, M. Schuchmann, P. R. Galle, H. Schulze-Bergkamen, Knockout of myeloid cell leukemia-1 induces liver damage and increases apoptosis susceptibility of murine hepatocytes. *Hepatology* **49**, 627–636 (2009).

20. C. D. DiNardo, K. Pratz, V. Pullarkat, B. A. Jonas, M. Arellano, P. S. Becker, O. Frankfurt, M. Konopleva, A. H. Wei, H. M. Kantarjian, T. Xu, W.-J. Hong, B. Chyla, J. Potluri, D. A. Pollyea, A. Letai, Venetoclax combined with decitabine or azacitidine in treatment-naive, elderly patients with acute myeloid leukemia. *Blood* **133**, 7–17 (2019).

21. A. H. Wei, S. A. Strickland Jr., J.-Z. Hou, W. Fiedler, T. L. Lin, R. B. Walter, A. Enjeti, I. S. Tiong, M. Savona, S. Lee, B. Chyla, R. Popovic, A. H. Salem, S. Agarwal, T. Xu, K. M. Fakouhi, R. Humerickhouse, W.-J. Hong, J. Hayslip, G. J. Roboz, Venetoclax combined with low-dose cytarabine for previously untreated patients with acute myeloid leukemia: Results from a phase Ib/II study. *J. Clin. Oncol.* **37**, 1277–1284 (2019s).

22. C. D. DiNardo, C. R. Rausch, C. Benton, T. Kadia, N. Jain, N. Pemmaraju, N. Daver, W. Covert, K. R. Marx, M. Mace, E. Jabbour, J. Cortes, G. Garcia-Manero, F. Ravandi, K. N. Bhalla, H. Kantarjian, M. Konopleva, Clinical experience with the BCL2-inhibitor venetoclax in combination therapy for relapsed and refractory acute myeloid leukemia and related myeloid malignancies. *Am. J. Hematol.* **93**, 401–407 (2018).

23. P. Blombery, M. A. Anderson, J. N. Gong, R. Thijssen, R. W. Birkinshaw, E. R. Thompson, C. E. Teh, T. Nguyen, Z. Xu, C. Flensburg, T. E. Lew, I. J. Majewski, D. H. D. Gray, D. A. Westerman, C. S. Tam, J. F. Seymour, P. E. Czabotar, D. C. S. Huang, A. W. Roberts, Acquisition of the recurrent Gly101Val mutation in BCL2 confers resistance to venetoclax in patients with progressive chronic lymphocytic leukemia. *Cancer Discov.* **9**, 342–353 (2019).

24. T. Hart, M. Chandrashekhar, M. Aregger, Z. Steinhart, K. R. Brown, G. MacLeod, M. Mis, M. Zimmermann, A. Fradet-Turcotte, S. Sun, P. Mero, P. Dirks, S. Sidhu, F. P. Roth, O. S. Rissland, D. Durocher, S. Angers, J. Moffat, High-resolution CRISPR screens reveal fitness genes and genotype-specific cancer liabilities. *Cell* **163**, 1515–1526 (2015).

25. W. Li, H. Xu, T. Xiao, L. Cong, M. I. Love, F. Zhang, R. A. Irizarry, J. S. Liu, M. Brown, X. S. Liu, MAGeCK enables robust identification of essential genes from genome-scale CRISPR/Cas9 knockout screens. *Genome Biol.* **15**, 554 (2014).

26. E. Cavdar Koc, A. Ranasinghe, W. Burkhart, K. Blackburn, H. Koc, A. Moseley, L. L. Spremulli, A new face on apoptosis: Death-associated protein 3 and PDCD9 are mitochondrial ribosomal proteins. *FEBS Lett.* **492**, 166–170 (2001).

27. H.-J. Kim, P. Maiti, A. Barrientos, Mitochondrial ribosomes in cancer. *Semin. Cancer Biol.* **47**, 67–81 (2017).

28. A. Rozanska, R. Richter-Dennerlein, J. Rorbach, F. Gao, R. J. Lewis, Z. M. Chrzanowska-Lightowlers, R. N. Lightowlers, The human RNA-binding protein RBFA promotes the maturation of the mitochondrial ribosome. *Biochem. J.* **474**, 2145–2158 (2017).

29. M. P. Luna-Vargas, J. E. Chipuk, The deadly landscape of pro-apoptotic BCL-2 proteins in the outer mitochondrial membrane. *FEBS J.* **283**, 2676–2689 (2016).

30. S. Flanagan, E. E. McKee, D. Das, P. M. Tulkens, H. Hosako, J. Fiedler-Kelly, J. Passarell, A. Radovsky, P. Prokocimer, Nonclinical and pharmacokinetic assessments to evaluate the potential of tedizolid and linezolid to affect mitochondrial function. *Antimicrob. Agents Chemother.* **59**, 178–185 (2014).

31. R. Lamb, B. Ozsvari, C. L. Lisanti, H. B. Tanowitz, A. Howell, U. E. Martinez-Outschoorn, F. Sotgia, M. P. Lisanti, Antibiotics that target mitochondria effectively eradicate cancer stem cells, across multiple tumor types: Treating cancer like an infectious disease. *Oncotarget* **6**, 4569–4584 (2015).

32. N. Moullan, L. Mouchiroud, X. Wang, D. Ryu, E. G. Williams, A. Mottis, V. Jovaisaite, M. V. Frochaux, P. M. Quiros, B. Deplancke, R. H. Houtkooper, J. Auwerx, Tetracyclines disturb mitochondrial function across eukaryotic models: A call for caution in biomedical research. *Cell Rep.* **10**, 1681–1691 (2015).

33. R. H. Houtkooper, L. Mouchiroud, D. Ryu, N. Moullan, E. Katsyuba, G. Knott, R. W. Williams, J. Auwerx, Mitonuclear protein imbalance as a conserved longevity mechanism. *Nature* **497**, 451–457 (2013).

34. P. Casara, J. Davidson, A. Claperon, G. Le Toumelin-Braizat, M. Vogler, A. Bruno, M. Chanrion, G. Lysiak-Auvity, T. Le Diguarher, J.-B. Starck, I. Chen, N. Whitehead, C. Graham, N. Matassova, P. Dokurno, C. Pedder, Y. Wang, S. Qiu, A.-M. Girard, E. Schneider, F. Gravé, A. Studeny, G. Guasconi, F. Rocchetti, S. Maïga, J.-M. Henlin, F. Colland, L. Kraus-Berthier, S. Le Gouill, M. J. S. Dyer, R. Hubbard, M. Wood, M. Amiot, G. M. Cohen, J. A. Hickman, J. Morris, J. Murray, O. Geneste, S55746 is a novel orally active BCL-2 selective and potent inhibitor that impairs hematological tumor growth. *Oncotarget* **9**, 20075–20088 (2018).

35. A. Reinisch, S. M. Chan, D. Thomas, R. Majeti, Biology and clinical relevance of acute myeloid leukemia stem cells. *Semin. Hematol.* **52**, 150–164 (2015).

36. E. R. Lechman, B. Gentner, S. W. K. Ng, E. M. Schoof, P. van Galen, J. A. Kennedy, S. Nucera, F. Ciceri, K. B. Kaufmann, N. Takayama, S. M. Dobson, A. Trotman-Grant, G. Krivdova, J. Elzinga, A. Mitchell, B. Nilsson, K. G. Hermans, K. Eppert, R. Marke, R. Isserlin, V. Voisin, G. D. Bader, P. W. Zandstra, T. R. Golub, B. L. Ebert, J. Lu, M. Minden, J. C. Y. Wang, L. Naldini, J. E. Dick, miR-126 Regulates distinct self-renewal outcomes in normal and malignant hematopoietic stem cells. *Cancer Cell* **29**, 214–228 (2016).

37. S. K. Bae, S. H. Yang, K. N. Shin, J. K. Rhee, M. Yoo, M. G. Lee, Pharmacokinetics of DA-7218, a new oxazolidinone, and its active metabolite, DA-7157, after intravenous and oral administration of DA-7218 and DA-7157 to rats. *J. Pharm. Pharmacol.* **59**, 955–963 (2007).

38. M. Zick, R. Rabl, A. S. Reichert, Cristae formation—linking ultrastructure and function of mitochondria. *Biochim. Biophys. Acta* **1793**, 5–19 (2009).

39. R. J. Youle, A. M. van der Bliek, Mitochondrial fission, fusion, and stress. *Science* **337**, 1062–1065 (2012).

40. B. Jhas, S. Sriskanthadevan, M. Skrtic, M. A. Sukhai, V. Voisin, Y. Jitkova, M. Gronda, R. Hurren, R. C. Laister, G. D. Bader, M. D. Minden, A. D. Schimmer, Metabolic adaptation to chronic inhibition of mitochondrial protein synthesis in acute myeloid leukemia cells. *PLOS ONE* **8**, e58367 (2013).

41. U. Richter, K. Y. Ng, F. Suomi, P. Marttinen, T. Turunen, C. Jackson, A. Suomalainen, H. Vihinen, E. Jokitalo, T. A. Nyman, M. A. Isokallio, J. B. Stewart, C. Mancini, A. Brusco, S. Seneca, A. Lombès, R. W. Taylor, B. J. Battersby, Mitochondrial stress response triggered by defects in protein synthesis quality control. *Life Sci. Alliance* **2**, e201800219 (2019).

42. S. K. Buchanan, J. E. Walker, Large-scale chromatographic purification of F1F0-ATPase and complex I from bovine heart mitochondria. *Biochem. J.* **318**, 343–349 (1996).

43. A. J. Y. Jones, J. N. Blaza, H. R. Bridges, B. May, A. L. Moore, J. Hirst, A self-assembled respiratory chain that catalyzes NADH oxidation by ubiquinone-10 cycling between complex I and the alternative oxidase. *Angew. Chem. Int. Ed.* **55**, 728–731 (2016).

44. E. Lapuente-Brun, R. Moreno-Loshuertos, R. Acín-Pérez, A. Latorre-Pellicer, C. Colás, E. Balsa, E. Perales-Clemente, P. M. Quirós, E. Calvo, M. A. Rodríguez-Hernández, P. Navas, R. Cruz, Á. Carracedo, C. López-Otín, A. Pérez-Martos, P. Fernández-Silva, E. Fernández-Vizarra, J. A. Enríquez, Supercomplex assembly determines electron flux in the mitochondrial electron transport chain. *Science* **340**, 1567–1570 (2013).

45. I. Lopez-Fabuel, J. Le Douce, A. Logan, A. M. James, G. Bonvento, M. P. Murphy, A. Almeida, J. P. Bolaños, Complex I assembly into supercomplexes determines differential mitochondrial ROS production in neurons and astrocytes. *Proc. Natl. Acad. Sci. U.S.A.* **113**, 13063–13068 (2016).

46. B. B. Seo, J. Wang, T. R. Flotte, T. Yagi, A. Matsuno-Yagi, Use of the NADH-quinone oxidoreductase (NDI1) gene of *Saccharomyces cerevisiae* as a possible cure for complex I defects in human cells. *J. Biol. Chem.* **275**, 37774–37778 (2000).

47. P. M. Quirós, M. A. Prado, N. Zamboni, D. D'Amico, R. W. Williams, D. Finley, S. P. Gygi, J. Auwerx, Multi-omics analysis identifies ATF4 as a key regulator of the mitochondrial stress response in mammals. *J. Cell Biol.* **216**, 2027–2045 (2017).

48. K. Pakos-Zebrucka, I. Koryga, K. Mnich, M. Ljujic, A. Samali, A. M. Gorman, The integrated stress response. *EMBO Rep.* **17**, 1374–1395 (2016).

49. P. D. Lu, H. P. Harding, D. Ron, Translation reinitiation at alternative open reading frames regulates gene expression in an integrated stress response. *J. Cell Biol.* **167**, 27–33 (2004).

50. M. Boitard, R. Bocchi, K. Egervari, G. Petrenko, B. Viale, S. Gremaud, E. Zgraggen, P. Salmon, J. Z. Kiss, Wnt signaling regulates multipolar-to-bipolar transition of migrating neurons in the cerebral cortex. *Cell Rep.* **10**, 1349–1361 (2015).

51. A. F. Zyryanova, F. Weis, A. Faille, A. A. Alard, A. Crespillo-Casado, Y. Sekine, H. P. Harding, F. Allen, L. Parts, C. Fromont, P. M. Fischer, A. J. Warren, D. Ron, Binding of ISRIB reveals a regulatory site in the nucleotide exchange factor eIF2B. *Science* **359**, 1533–1536 (2018).

52. J. C. Tsai, L. E. Miller-Vedam, A. A. Anand, P. Jaishankar, H. C. Nguyen, A. R. Renslo, A. Frost, P. Walter, Structure of the nucleotide exchange factor eIF2B reveals mechanism of memory-enhancing molecule. *Science* **359**, eaaq0939 (2018).

53. S. R. Stockwell, G. Platt, S. E. Barrie, G. Zoumpoulidou, R. H. te Poele, G. W. Aherne, S. C. Wilson, P. Sheldrake, E. McDonald, M. Venet, C. Soudy, F. Elustondo, L. Rigoreau, J. Blagg, P. Workman, M. D. Garrett, S. Mittnacht, Mechanism-based screen for G1/S checkpoint activators identifies a selective activator of EIF2AK3/PERK signalling. *PLOS ONE* **7**, e28568 (2012).

Sharon *et al.*, *Sci. Transl. Med.* **11**, eaax2863 (2019)   30 October 2019

14 of 15

54. H. Bai, T. Chen, J. Ming, H. Sun, P. Cao, D. N. Fusco, R. T. Chung, M. Chorev, Q. Jin, B. H. Aktas, Dual activators of protein kinase R (PKR) and protein kinase R-like kinase PERK identify common and divergent catalytic targets. *Chembiochem* **14**, 1255–1262 (2013).

55. M. Boyce, K. F. Bryant, C. Jousse, K. Long, H. P. Harding, D. Scheuner, R. J. Kaufman, D. Ma, D. M. Coen, D. Ron, J. Yuan, A selective inhibitor of eIF2α dephosphorylation protects cells from ER stress. *Science* **307**, 935–939 (2005).

56. H. Puthalakath, L. A. O'Reilly, P. Gunn, L. Lee, P. N. Kelly, N. D. Huntington, P. D. Hughes, E. M. Michalak, J. McKimm-Breschkin, T. Motoyama, S. Gotoh, S. Akira, P. Bouillet, A. Strasser, ER stress triggers apoptosis by activating BH3-only protein Bim. *Cell* **129**, 1337–1349 (2007).

57. R. M. Fritsch, G. Schneider, D. Saur, M. Scheibel, R. M. Schmid, Translational repression of MCL-1 couples stress-induced eIF2α phosphorylation to mitochondrial apoptosis initiation. *J. Biol. Chem.* **282**, 22551–22562 (2007).

58. W. Lieberthal, S. A. Menza, J. S. Levine, Graded ATP depletion can cause necrosis or apoptosis of cultured mouse proximal tubular cells. *Am. J. Physiol.* **274**, F315–F327 (1998).

59. S. D. Flanagan, P. A. Bien, K. A. Muñoz, S. L. Minassian, P. G. Prokocimer, Pharmacokinetics of tedizolid following oral administration: Single and multiple dose, effect of food, and comparison of two solid forms of the prodrug. *Pharmacotherapy* **34**, 240–250 (2014).

60. G. L. Drusano, W. Liu, R. Kulawy, A. Louie, Impact of granulocytes on the antimicrobial effect of tedizolid in a mouse thigh infection model. *Antimicrob. Agents Chemother.* **55**, 5300–5305 (2011).

61. M. von Bonin, M. Wermke, K. N. Cosgun, C. Thiede, M. Bornhauser, G. Wagemaker, C. Waskow, In vivo expansion of co-transplanted T cells impacts on tumor re-initiating activity of human acute myeloid leukemia in NSG mice. *PLOS ONE* **8**, e60680 (2013).

62. C. D. DiNardo, K. W. Pratz, A. Letai, B. A. Jonas, A. H. Wei, M. Thirman, M. Arellano, M. G. Frattini, H. Kantarjian, R. Popovic, B. Chyla, T. Xu, M. Dunbar, S. K. Agarwal, R. Humerickhouse, M. Mabry, J. Potluri, M. Konopleva, D. A. Pollyea, Safety and preliminary efficacy of venetoclax with decitabine or azacitidine in elderly patients with previously untreated acute myeloid leukaemia: A non-randomised, open-label, phase 1b study. *Lancet Oncol.* **19**, 216–228 (2018).

63. T. V. Milosevic, V. L. Payen, P. Sonveaux, G. G. Muccioli, P. M. Tulkens, F. Van Bambeke, Mitochondrial alterations (inhibition of mitochondrial protein expression, oxidative metabolism, and ultrastructure) induced by linezolid and tedizolid at clinically relevant concentrations in cultured human HL-60 promyelocytes and THP-1 monocytes. *Antimicrob. Agents Chemother.* **62**, e01599-17 (2018).

64. M. P. Crotty, T. Krekel, C. A. Burnham, D. J. Ritchie, New gram-positive agents: The next generation of oxazolidinones and lipoglycopeptides. *J. Clin. Microbiol.* **54**, 2225–2232 (2016).

65. M. Ravà, A. D'Andrea, P. Nicoli, I. Gritti, G. Donati, M. Doni, M. Giorgio, D. Olivero, B. Amati, Therapeutic synergy between tigecycline and venetoclax in a preclinical model of MYC/ BCL2 double-hit B cell lymphoma. *Sci. Transl. Med.* **10**, eaan8723 (2018).

66. E. D. Lagadinou, A. Sach, K. Callahan, R. M. Rossi, S. J. Neering, M. Minhajuddin, J. M. Ashton, S. Pei, V. Grose, K. M. O'Dwyer, J. L. Liesveld, P. S. Brookes, M. W. Becker, C. T. Jordan, BCL-2 inhibition targets oxidative phosphorylation and selectively eradicates quiescent human leukemia stem cells. *Cell Stem Cell* **12**, 329–341 (2013).

67. L. Xiong, Y. Tang, Z. Liu, J. Dai, X. Wang, BCL-2 inhibition impairs mitochondrial function and targets oral tongue squamous cell carcinoma. *SpringerPlus* **5**, 1626 (2016).

68. F. Lucantoni, H. Dussmann, I. Llorente-Folch, J. H. M. Prehn, BCL2 and BCL(X)L selective inhibitors decrease mitochondrial ATP production in breast cancer cells and are synthetically lethal when combined with 2-deoxy-D-glucose. *Oncotarget* **9**, 26046–26063 (2018).

69. D. A. Pollyea, B. M. Stevens, C. L. Jones, A. Winters, S. Pei, M. Minhajuddin, A. D'Alessandro, R. Culp-Hill, K. A. Riemondy, A. E. Gillen, J. R. Hesselberth, D. Abbott, D. Schatz, J. A. Gutman, E. Purev, C. Smith, C. T. Jordan, Venetoclax with azacitidine disrupts energy metabolism and targets leukemia stem cells in patients with acute myeloid leukemia. *Nat. Med.* **24**, 1859–1866 (2018).

70. G. Karpel-Massler, M. Bâ, C. Shu, M.-E. Halatsch, M.-A. Westhoff, J. N. Bruce, P. Canoll, M. D. Siegelin, TIC10/ONC201 synergizes with Bcl-2/Bcl-xL inhibition in glioblastoma by suppression of Mcl-1 and its binding partners in vitro and in vivo. *Oncotarget* **6**, 36456–36471 (2015).

71. K. Crassini, Y. Shen, W. S. Stevenson, R. Christopherson, C. Ward, S. P. Mulligan, O. G. Best, MEK1/2 inhibition by binimetinib is effective as a single agent and potentiates the actions of Venetoclax and ABT-737 under conditions that mimic the chronic lymphocytic leukaemia (CLL) tumour microenvironment. *Br. J. Haematol.* **182**, 360–372 (2018).

72. P. van Galen, N. Mbong, A. Kreso, E. M. Schoof, E. Wagenblast, S. W. K. Ng, G. Krivdova, L. Jin, H. Nakauchi, J. E. Dick, Integrated stress response activity marks stem cells in normal hematopoiesis and leukemia. *Cell Rep.* **25**, 1109–1117.e5 (2018).

73. C. L. Jones, B. M. Stevens, A. D'Alessandro, J. A. Reisz, R. Culp-Hill, T. Nemkov, S. Pei, N. Khan, B. Adane, H. Ye, A. Krug, D. Reinhold, C. Smith, J. DeGregori, D. A. Pollyea, C. T. Jordan, Inhibition of amino acid metabolism selectively targets human leukemia stem cells. *Cancer Cell* **34**, 724–740.e4 (2018).

Sharon *et al.*, *Sci. Transl. Med.* **11**, eaax2863 (2019)   30 October 2019

15 of 15

Science Translational Medicine

Inhibition of mitochondrial translation overcomes venetoclax resistance in AML through activation of the integrated stress response

David Sharon, Severine Cathelin, Sara Mirali, Justin M. Di Trani, David J. Yanofsky, Kristine A. Keon, John L. Rubinstein, Aaron D. Schimmer, Troy Ketela and Steven M. Chan

Triple threat for leukemia

Acute myeloid leukemia is a relatively common and aggressive cancer with few good therapeutic options thus far. Venetoclax, a drug that promotes apoptosis, has shown some promise in this disease, but it has been limited by the development of resistance. Using a high-throughput screen, Sharon *et al.* determined that ribosome-targeting antibiotics such as tedizolid can help overcome venetoclax resistance by suppressing mitochondrial respiration and activating the cellular stress response. The combination was even more effective with the addition of the epigenetic drug azacitidine, both in vitro and in mouse models of leukemia, suggesting the translational potential of these treatments.

ARTICLE TOOLS	http://stm.sciencemag.org/content/11/516/eaax2863
SUPPLEMENTARY MATERIALS	http://stm.sciencemag.org/content/suppl/2019/10/28/11.516.eaax2863.DC1
RELATED CONTENT	http://stm.sciencemag.org/content/scitransmed/11/508/eaaw8828.full http://stm.sciencemag.org/content/scitransmed/10/436/eaao3003.full http://stm.sciencemag.org/content/scitransmed/10/431/eaam8460.full http://stm.sciencemag.org/content/scitransmed/9/413/eaao1214.full
REFERENCES	This article cites 73 articles, 31 of which you can access for free http://stm.sciencemag.org/content/11/516/eaax2863#BIBL
PERMISSIONS	http://www.sciencemag.org/help/reprints-and-permissions

Use of this article is subject to the Terms of Service